Reviewed Preprint
v1 • February 5, 2025
Not revised

Reviewed Preprint
v2 • March 16, 2026
Revised by authors

# Increased reluctant vesicles underlie synaptic depression by GPR55 in axon terminals of cerebellar Purkinje cells

**Takuma Inoshita, Shin-ya Kawaguchi**
Department of Biophysics, Graduate School of Science, Kyoto University Oiwake-cho, Kyoto, Japan

**For correspondence:**
kawaguchi@nb.biophys.kyoto-u.ac.jp

**Competing interests:** No competing interests declared

**Funding:** See page 24

**Reviewing editor:** Katalin Toth, University of Ottawa, Canada



## eLife Assessment

This is an **important** study reporting that activation of the presynaptic GPR55 receptor suppresses synaptic transmission by modulating GABA release through the reduction of the readily releasable pool without affecting the presynaptic AP waveform and calcium influx. The evidence supporting this claim is **compelling** and based on an impressive array of techniques including patch-clamp recordings from the axon terminals of cerebellar Purkinje cells and fluorescent imaging of vesicular exocytosis. While the authors have strengthened their conclusions on several technical fronts in the revised version, further investigation is needed into the mechanism by which GPR55 activation might make vesicles insensitive to the rise in presynaptic [$Ca^{2+}$] mediated by VGCCs, and the nature of the endogenous process that would activate this pathway in vivo.

https://doi.org/10.7554/eLife.105268.2.sa4

## Abstract

Control of synaptic transmission efficacy by neuronal activity and neuromodulators is pivotal for brain function. Synaptic suppression by cannabinoids activating CB1 receptors has been extensively studied at the molecular and cellular levels to understand the neuronal basis for effects of cannabis intake. Here, we focused on GPR55, non-canonical type of cannabinoid receptor, which shows sensitivity to cannabidiol included in cannabis, aiming to highlight its actions on presynaptic function. Taking advantage of direct patch-clamp recordings from axon terminals of cerebellar Purkinje cells together with fluorescent imaging of vesicular exocytosis using synapto-pHluorin, we show that GPR55 suppresses synaptic transmission as CB1 receptor does, but through a distinct presynaptic modulation of release machinery. Activation of GPR55 reduced transmitter release by changing neither presynaptic action potential waveform nor $Ca^{2+}$ influx, but by making a large population of $Ca^{2+}$-responsive synaptic vesicles insensitive to $Ca^{2+}$ influx through voltage-gated $Ca^{2+}$ channels, leading to substantial reduction of the readily releasable pool of vesicles. Thus, the present study identifies a unique mechanism to suppress presynaptic transmitter release by an atypical cannabinoid receptor GPR55, which would enable subtype-specific modulation of neuronal computation by cannabinoid receptors.

## Introduction

Neuronal communication at chemical synapses is central to information processing in the circuit, and its activity-dependent modulation provides adaptive change of brain computation (Kandel, 2001). Short- and long-term changes of transmission efficacy at central synapses have been extensively studied in terms of molecular/cellular mechanisms and physiological significance, which have demonstrated their critical roles in learning and memory in animals (Abbott and Regehr, 2004). One of such modulations of synaptic strength is that by endocannabinoids (Kreitzer and Regehr, 2001; Ohno-Shosaku et al., 2001; Wilson and Nicoll, 2001; Diana et al., 2002), which is also related to the cellular and neuronal basis for actions of cannabis (Kano et al., 2009). One well-known synaptic modulation by cannabinoids is the activity-dependent short-

term suppression of synaptic transmission, such as depolarization-induced suppression of excitation (DSE) and inhibition (DSI), caused by reduced transmitter release from presynaptic terminals as a result of activation of cannabinoid receptor type 1 (CB1). The CB1 receptor activation is thought to decrease presynaptic $Ca^{2+}$ influx upon an action potential (AP) arrival (Kreitzer and Regehr, 2001; Kushmerick et al., 2004; Wu et al., 2020).

In spite of the substantial efforts that have been made for unraveling cannabinoids' action on the nervous system, it still remains elusive whether the reduction of $Ca^{2+}$ influx fully explains the suppression of transmission by cannabinoids or other mechanisms, such as altered release machinery, may also be involved generally at central synapses, as already suggested for CB1-mediated change of presynaptic vesicular docking (Ramírez-Franco et al., 2014). In addition, multiple types of molecules contained in cannabis are now known to act on the nervous system, and particularly one of them, cannabidiol, is attracting attention because of its potential preferred therapeutic actions on various neurological dysfunctions such as epilepsy and anxiety symptoms (Shallcross et al., 2019; Devinsky et al., 2024). GPR55, a cannabinoid receptor that has been identified as a potential target of cannabidiol (Baker et al., 2006; Oka et al., 2007), was recently reported to modulate synaptic transmission at glutamatergic and GABAergic synapses in the hippocampus (Sylantyev et al., 2013; Rosenberg et al., 2023), although the detailed mechanism of action remains unclear. GPR55, unlike typical cannabinoid receptors such as CB1 receptors that couple to $G_i$ proteins, interacts with multiple G proteins including $G\alpha_q$ and $G\alpha_{13}$, thereby activating downstream pathways such as phospholipase C (PLC)/$IP_3$-mediated $Ca^{2+}$ signaling and RhoA/ROCK-dependent cytoskeletal modulation (Henstridge et al., 2010; Balenga et al., 2011). This distinct signaling profile suggests that GPR55 is likely to regulate synaptic transmission through a mechanism different from CB1 receptor.

To study in detail how cannabinoids modulate synaptic physiology, direct *tour-de-force* patch-clamp recording of transmitter release at axon terminals, in combination with molecular biological methods and fluorescent imaging, would be a powerful technique. One preparation that is amenable to detailed biophysical analysis of transmitter release is the axon terminals of cerebellar Purkinje cells (PCs) (Kawaguchi and Sakaba, 2015), which are expected to express GPR55 based on data from in situ hybridization, RT-PCR and immunolabeling (Ryberg et al., 2007; Wu et al., 2013), although its subcellular localization remains unclear. Taking advantage of the feasibility to perform direct patch-clamp recording from axon terminals in combination with fluorescent imaging of vesicular fusion in dissociated cultures, and postsynaptic recordings from neurons in deep cerebellar nuclei (DCN) of slices, here we studied how the presynaptic release machinery is modulated by GPR55. Here, we demonstrate that GPR55 is present at PC axon terminals and suppresses synaptic transmission through a unique modulatory action: GPR55 increases reluctant vesicles by depriving the sensitivity to APs.

# Results

## GPR55 inhibits synaptic transmission at PC output synapses

We first examined the role of GPR55 in synaptic transmission from a PC in acute cerebellar slices. Cerebellar sagittal slices were prepared from postnatal day (P)28-35 rats, and whole-cell patch-clamp recordings were performed from neurons with large cell bodies (> 15 μm diameter) in the DCN (Figure 1A; Uusisaari et al., 2006). The DCN neurons were voltage-clamped at -70 to -100 mV, and evoked IPSCs (eIPSCs) were recorded following electrical stimulation at the white matter in the presence of an AMPA receptor antagonist, NBQX (10 μM). In accord with previous studies (Kawaguchi and Sakaba, 2015), eIPSCs at PC-DCN synapses were identified by the sudden appearance of large amplitude responses (2.04 ± 0.48 nA) in an almost all-or-none manner as stimulation intensity was increased (Figure 1B). Bath application of a GPR55 agonist, AM251 (5 μM; $EC_{50}$ = 39 nM assayed in HEK cells; Ryberg et al., 2007; Henstridge et al., 2009) decreased the amplitude of eIPSCs (69.1 ± 5.1% at +5 min, p = 0.00226, compared with -1 min, paired t-test), accompanied by an increase in the coefficient of variation (CV) of the responses (156.0 ± 19.8% at +5 min, p = 0.0490) (Figure 1B, C). Increase in the CV is typically interpreted as a lowered presynaptic release probability. These results suggest that GPR55 suppresses synaptic transmission

at PC-DCN synapses, similarly to what CB1 receptor does at other synapses (Kreitzer and Regehr, 2001; Ohno-Shosaku et al., 2001; Wilson and Nicoll, 2001; Diana et al., 2002). Aiming at much more detailed analysis of synaptic function based on the feasibility to perform direct patch-clamp recordings from axon terminals, we also tested the action of GPR55 on PC outputs using the primary culture preparation. To fluorescently visualize PCs, we used an adeno-associated virus (AAV) vector, AAV2-CA-EGFP that preferentially infects PCs among cerebellar neurons, as in previous studies (Kawaguchi and Sakaba, 2015). Simultaneous whole-cell somatic patch-clamp recordings were performed from a presynaptic PC and its postsynaptic neuron (possible DCN neuron) surrounded by lots of EGFP-positive PC boutons, in the presence of NBQX (10 μM) (Figure 1D). Presynaptic PCs were voltage-clamped at -70 mV, and $Na^+$ current escaping as an AP from the patched soma to the axon was elicited by applying a voltage pulse (to 0 mV, 1~5 ms), which evoked IPSCs in the voltage-clamped postsynaptic target cell. In line with the data obtained in slices, synaptic transmission decreased upon GPR55 activation with AM251 (300 nM), manifested as a decrease in IPSC amplitudes (42.9 ± 8.0% at +5 min, p = 0.0134) and an increase in the CV (147.6 ± 14.7% at +5 min, p = 0.0431) (Figure 1E, I). The effect of AM251 became evident a few minutes after application, and somehow reached a saturated level within 5 minutes in both slice and culture preparations. It should be noted that AM251 is known to act not only as a GPR55 agonist, but also as an inverse agonist for CB1 (Ryberg et al., 2007; Henstridge et al., 2009). To confirm that the effect of AM251 is not due to the CB1 receptor inhibition, we also tested AM281, a CB1-specific inverse agonist. Application of AM281 (500 nM) did not induce any significant changes in eIPSC amplitude or its CV (amplitude: 97.8 ± 3.6% at +5 min, p = 0.737; CV: 102.1 ± 7.5% at +5 min, p = 0.260) (Figure 1F, I), suggesting that the synaptic depression caused by AM251 is not due to CB1 receptor inhibition. Considering a previous study showing that PC synapses exhibit no modulation by CB1 receptors (Hirono and Yanagawa, 2021; see also Figure 1F, I), the effects of AM251 on synaptic outputs from a PC bouton seemed to be ascribed to activation of GPR55. Indeed, the suppressive effect of AM251 on synaptic transmission was abolished by a GPR55 antagonist CID16020046 (CID, 5 μM; $IC_{50}$ = 0.21 μM, specific for GPR55 without affecting CB1 receptor) (amplitude: 101.9 ± 16.4% at +5 min, p = 0.949; CV: 104.1 ± 13.1% at +5 min, p = 0.624) (Figure 1G, I). In addition, we also tested another GPR55 ligand, lysophosphatidylinositol (LPI, 1 μM; $EC_{50}$ = 30 nM, Oka et al., 2007), which is known as an endogenous ligand of GPR55 (Oka et al., 2007; Henstridge et al., 2009). Several types of LPI are known, and here we used soy-derived LPI (Merck, containing approximately 58% C16:0 and 42% C18:0 or C18:2), which was shown to activate GPR55 for synaptic modulation in the hippocampus (Rosenberg et al., 2023). As shown in Figure 1H and I, similar reduction of eIPSC amplitude and increase in its CV to those by AM251 were observed after the extracellular application of LPI (amplitude: 57.2 ± 4.6% at +5 min, p = 0.00111; CV: 141.2 ± 3.6% at +5 min, p = 0.00292). Neither application of AM251 nor LPI changed the time courses of IPSCs (AM251, 20-80% risetime: 0.81 ± 0.05 to 0.77 ± 0.04 ms, p = 0.296; LPI, 0.71 ± 0.10 to 0.65 ± 0.12 ms, p = 0.222) (Figure 1—figure supplement 1A) and presynaptic $Na^+$ currents recorded at the PC soma (AM251, 3.30 ± 0.33 to 3.25 ± 0.40 nA, p = 0.520; LPI, 2.87 ± 0.30 to 2.89 ± 0.31 nA, p = 0.728) (Figure 1—figure supplement 1B, C). Taken all these results based on pharmacological agents for GPR55 together, it was suggested that synaptic transmission is negatively regulated by GPR55 at synapses formed by PC axon terminals, presumably acting on the presynaptic side.

It is a critical issue to examine the presence of GPR55 at PC axon terminals. To address this, we attempted to fluorescently label neurons in cerebellar culture with molecules targeting GPR55, using a fluorescent derivative of AM251, Tocrifluor T1117 (T1117; Daly et al., 2010; Sylantyev et al., 2013; He et al., 2024). As shown in Figure 2A and B, confocal fluorescent images of GFP-positive PC axons and terminals clearly showed significant T1117 signal after incubation with T1117 (20 nM) for 2 min, which was selectively suppressed by the CRISPR/Cas9-mediated acute knock-down of GPR55 expression (relative fluorescence density of T1117, mean ± SD: control, 1.00 ± 0.49; GPR55-KD, 0.53 ± 0.27, p < 0.001; Cas9-alone, 1.04 ± 0.47, p = 0.493, compared with control, Dunnett's test) (Figure 2C; see Methods for details of the CRISPR/Cas9 knock-down). Thus, T1117 signals at PC axon terminals would be ascribed at least partially to GPR55. It should be noted that PC boutons showed marked deviation in the T1117 fluorescence intensity, probably reflecting

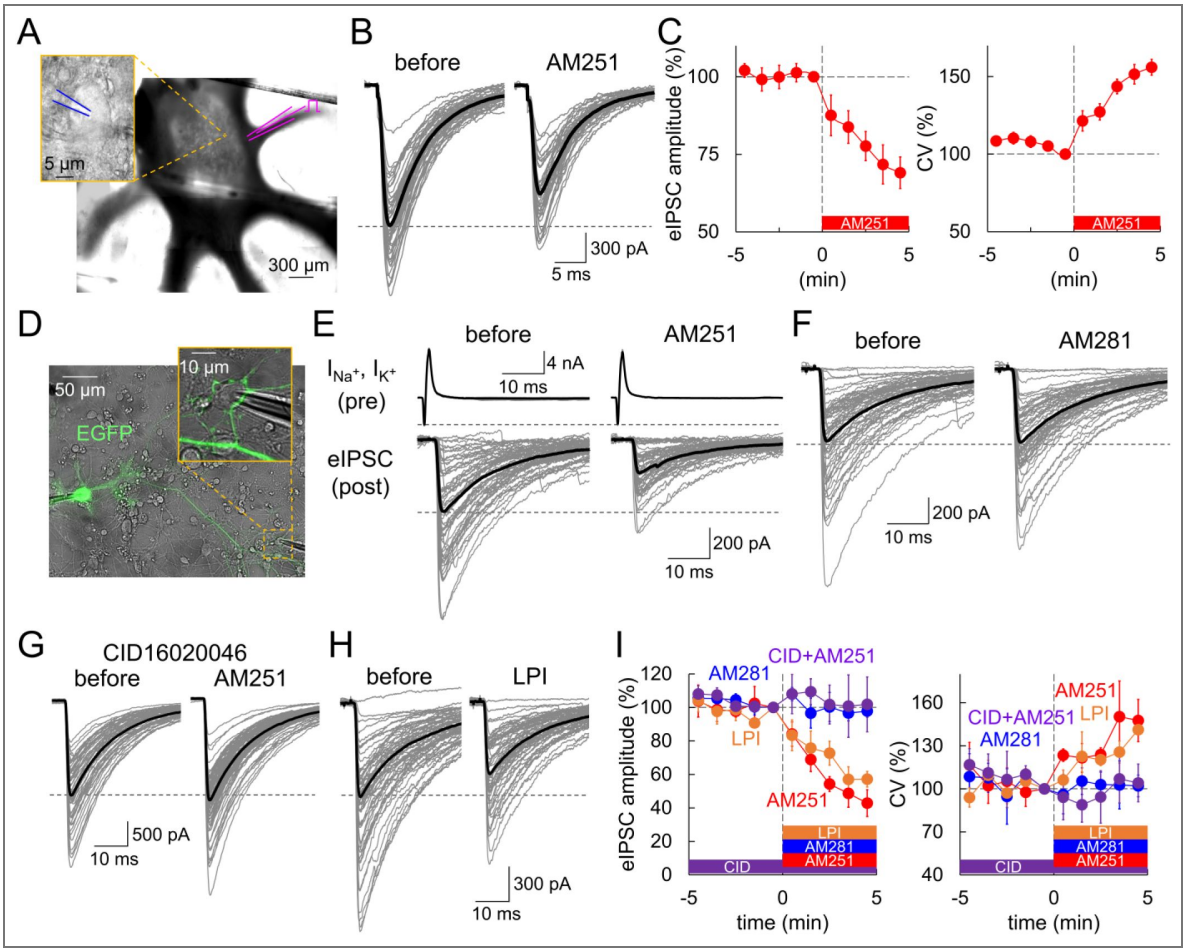


**Figure 1. Reduced transmission at PC-DCN synapses by GPR55 in slice and culture**

(**A**) Image of patch-clamp recording from a DCN neuron in slice. A magnified image of the recorded neuron is shown as an inset (a patch pipette is indicated in blue). A pipette for electrical stimulation (magenta) was placed at the white matter. (**B, C**) Individual (gray) and averaged (black) traces (B), and time courses of eIPSC amplitude (C, left) and CV (C, right) before and after the AM251 application (at time 0), n = 6. (**D**) Image of dual whole-cell recordings from a presynaptic EGFP-labeled PC soma and its postsynaptic target neuron in culture. (**E-H**) Representative traces of eIPSCs before and 5 minutes after the application of AM251 (E), AM281 (F), AM251 in the presence of CID (G), or LPI (H). In E, presynaptic $Na^+$ and the following $K^+$ currents ($I_{Na+}$, $I_{K+}$) at a presynaptic PC soma are also shown. (**I**) Time courses of eIPSC amplitude and CV. n = 6 (AM251), 5 (AM281), 5 (CID + AM251) and 5 cells (LPI). CID was applied from the beginning of the recording. The internal solution contained 0.5 mM EGTA. Data are shown as mean ± SEM.

variable GPR55 abundance at individual PC boutons. In addition, T1117 signals were also evident at GFP-negative structures (see Figure 2), probably due to labeling of axons/terminals of neurons such as granule cells and inhibitory interneurons which are well-known to potently express CB1 (Tsou et al., 1998), which is antagonized by AM251. Indeed, GFP-negative structures neighboring the GPR55-knocked down GFP-positive PC boutons showed clear T1117 signals (Figure 2B, C). The above results showing PC terminals labeled with a fluorescent AM251 analogue depending on the GPR55 gene expression indicated the presence of GPR55 with variable density at individual PC boutons, supporting the idea about modulation of PC output synapses by GPR55 (see Figure 1).

## GPR55 suppresses transmitter release in PC boutons without changing presynaptic $Ca^{2+}$ influx

Taking advantage of the feasibility to directly patch-clamp record from GPR55-expressing PC axon terminals (Kawaguchi and Sakaba, 2015), we next attempted to examine the mechanism how GPR55 suppresses the transmission. One candidate mechanism is the reduction of the presynaptic $Ca^{2+}$ influx, as CB1 does at the calyx of Held synapses and climbing fiber synapses on PCs (Kreitzer and Regehr, 2001; Kushmerick et al., 2004; Wu et al., 2020). To record presynaptic $Ca^{2+}$ current, direct voltage-clamp recordings were performed from PC boutons (Figure 3A). Concomitantly, we also monitored the membrane capacitance ($C_m$) increase ($\Delta C_m$) caused by the $Ca^{2+}$ influx, which is an indication of the amount of exocytosed synaptic vesicles. Unexpectedly, $Ca^{2+}$ currents induced by square depolarizing pulses (0 mV for 5 ms) were not affected by AM251 in the voltage-clamped PC boutons (53.0 ± 5.6 to 52.4 ± 6.3 pA/pF, p = 0.808), whereas the resultant increase in $C_m$ was markedly diminished (22 ± 4 to 13 ± 2 fF/pF, p = 0.0448) (Figure 3B, C). This strong reduction of vesicle exocytosis by AM251 was mediated by GPR55, as evidenced by its abolishment by the knock-down of GPR55 expression using CRISPR/Cas9 system without any effects on presynaptic $Ca^{2+}$ influx (Figure 3D, E; $Ca^{2+}$ current: Cas9 alone, 55.1 ± 9.8 to 54.7 ± 9.6 pA/pF, p = 0.715, paired t-test; GPR55-KD, 56.7 ± 10.0 to 54.7 ± 9.8 pA/pF, p = 0.176; $\Delta C_m$: Cas9 alone, 28 ± 1 to 15 ± 1 fF/pF, p < 0.001; GPR55-KD, 27 ± 5 to 24 ± 6 fF/pF, p = 0.174). Taken together, our direct patch-clamp recordings from PC terminals indicated potent suppression of vesicle exocytosis by GPR55 without changing $Ca^{2+}$ influx, which is distinct from the typical synaptic modulation by CB1 receptors through a reduction of presynaptic $Ca^{2+}$ influx.

We further tested whether GPR55 also affects APs and postsynaptic $GABA_A$ receptor responsiveness at PC-DCN synapses. Previous studies demonstrated that AP waveforms are subject to modulation in PC axons in a manner dependent on high frequency firing, local activation of axonal transmitter receptors, and/or intracellular cAMP changes (Kawaguchi and Sakaba, 2015; Zorrilla de San Martin et al., 2017; Furukawa et al., 2024). To test the possibility of a change in the AP waveform by GPR55, we performed direct patch-clamp recordings of APs from a presynaptic bouton of a PC axon (Figure 4A). As shown in Figure 4B and C, current-clamp recordings from the axon terminals detected no changes of APs by GPR55 in both the amplitude and time course (amplitude: 91.2 ± 7.5 to 90.4 ± 6.4 mV, p = 0.701, paired t-test; half-width: 0.54 ± 0.06 to 0.54 ± 0.07 ms, p = 0.832). In terms of modulation of postsynaptic responsiveness by GPR55, decrease in accumulation of postsynaptic $GABA_A$ receptors at hippocampal GABAergic synapses was suggested (Khan A. et al., 2018; Rosenberg et al., 2023). However, miniature IPSCs (mIPSCs) recorded from a postsynaptic DCN cell innervated by lots of EGFP-labeled PC boutons in the presence of TTX (1 μM) and NBQX (10 μM) (Figure 4D and Figure4—figure supplement 1) showed no change in either amplitude or frequency after the AM251 application (amplitude: 101.5 ± 9.7% at +5 min, p = 0.941; frequency: 85.4 ± 13.4%, p = 0.608) (Figure 4E, F). Together, these results demonstrated that GPR55 suppresses transmitter release from PC boutons not by altering presynaptic $Ca^{2+}$ influx, AP waveforms, or postsynaptic responsiveness, but rather by directly reducing vesicle exocytosis.

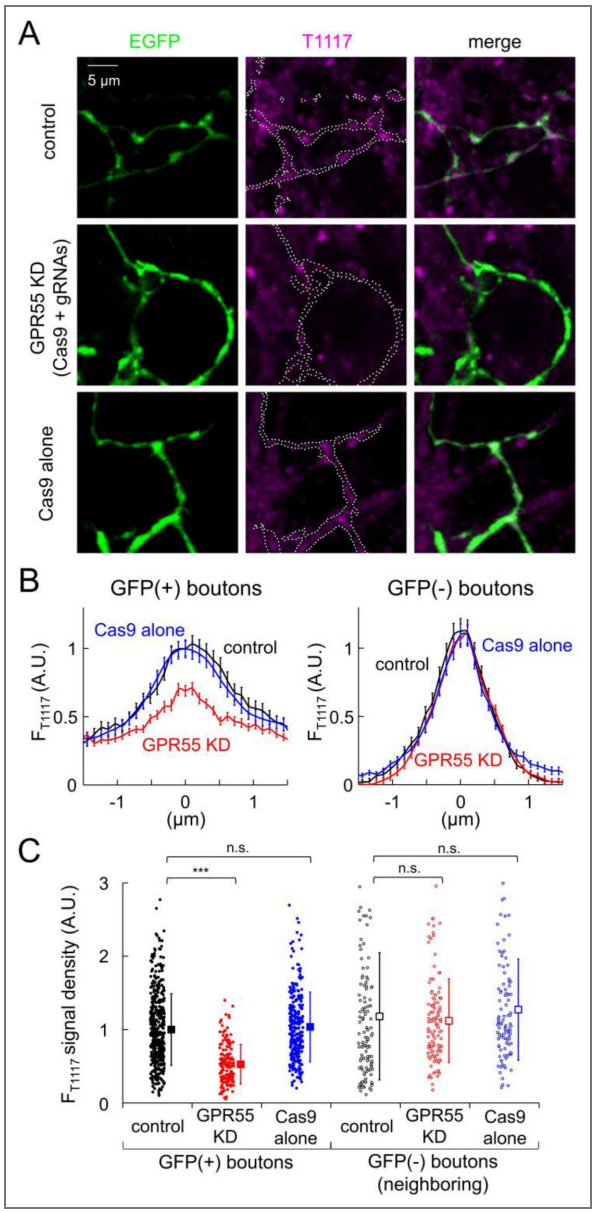


**Figure 2. Localization of GPR55 at PC axonal boutons**

(**A**) Representative confocal fluorescent images of GFP and T1117 labeling in control and transfected cells with GPR55-targeting CRISPR/Cas9 vectors or Cas9-alone. White dotted lines in the T1117 images indicate the outlines of GFP-labeled axons. (**B**) Spatial profiles of T1117 signals in GFP(+) or GFP(-) boutons. Averaged data are shown as mean ± SEM. Fluorescence peak of GFP (for GFP(+) boutons) or T1117 (for GFP(-) boutons) was aligned to the position 0. (**C**) $F_{T1117}$ signal density (averaged fluorescence per pixel) in GFP(+) boutons (control, 455; GPR55-KD, 161; Cas9-alone, 270 boutons) or that in GFP(-) boutons near GFP(+) ones (control, 124; GPR55-KD, 116; Cas9-alone, 104 boutons). Data for individual boutons (circles) and mean ± SD (squares) are shown. ***, $p < 0.001$; n.s., not significant.

**Figure 3.** **Reduced vesicle exocytosis by GPR55 without changing presynaptic $Ca^{2+}$ influx**

(A) Image of direct patch-clamp recording from an EGFP-labeled PC axon terminal in culture. (**B-E**) Representative traces (B, D) and amplitude of presynaptic $Ca^{2+}$ currents during 5 ms depolarization ($I_{Ca2+}$) and the resultant $C_m$ increase ($\Delta C_m$, C, E) before and after the AM251 application in wild-type (n = 6) (B, C) or transfected cells with Cas9-alone (n = 5), or CRISPR/Cas9 for GPR55 (n = 6) (D, E). Both $I_{Ca2+}$ and $\Delta C_m$ were normalized by the size of presynaptic $C_m$ under the voltage-clamp. The internal solution contained 0.5 mM EGTA. Data are mean ± SEM. * p < 0.05; *** p < 0.001; n.s., not significant.

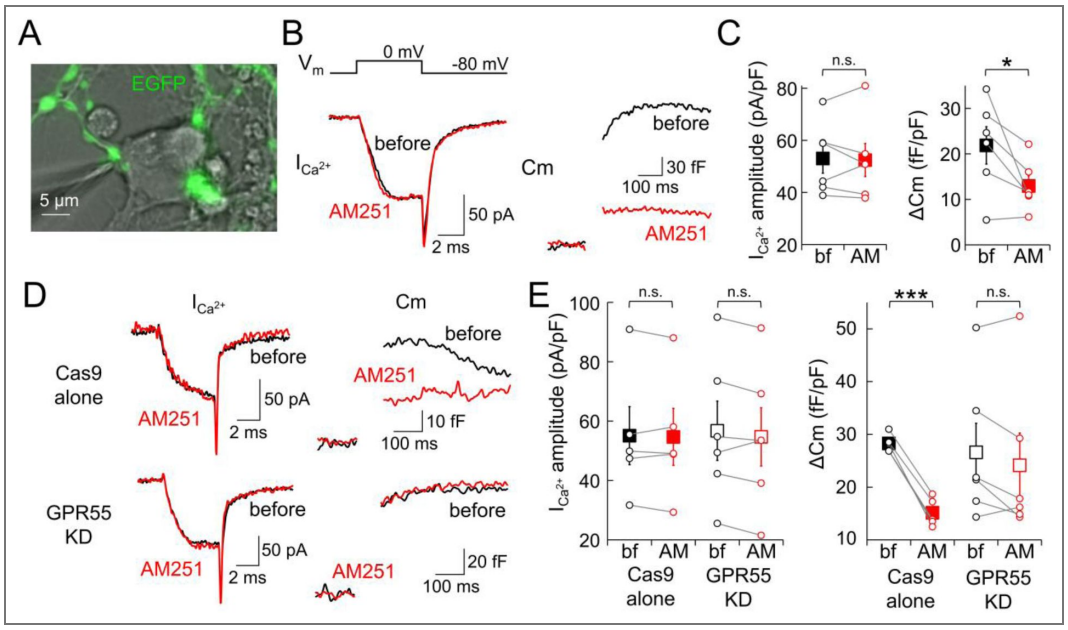


**Figure 4.** **GPR55 has no effect on APs or postsynaptic responsiveness**

(**A**) Image of direct recording from an EGFP-labeled PC axon terminal in culture. (**B, C**) Representative traces (B), amplitude and half-width (C) of APs recorded from PC terminals before and 5 minutes after the AM251 application (n = 5). (**D**) Image of mIPSC recordings from a neuron innervated by lots of EGFP-positive PC boutons in culture. (**E**) Representative traces of mIPSCs before and 5 minutes after the AM251 application. (**F**) Time courses of mIPSC amplitude and frequency (n = 4). At 0 min, AM251 was applied. The internal solution contained 0.5 mM EGTA. Data are shown as mean ± SEM. n.s., not significant.

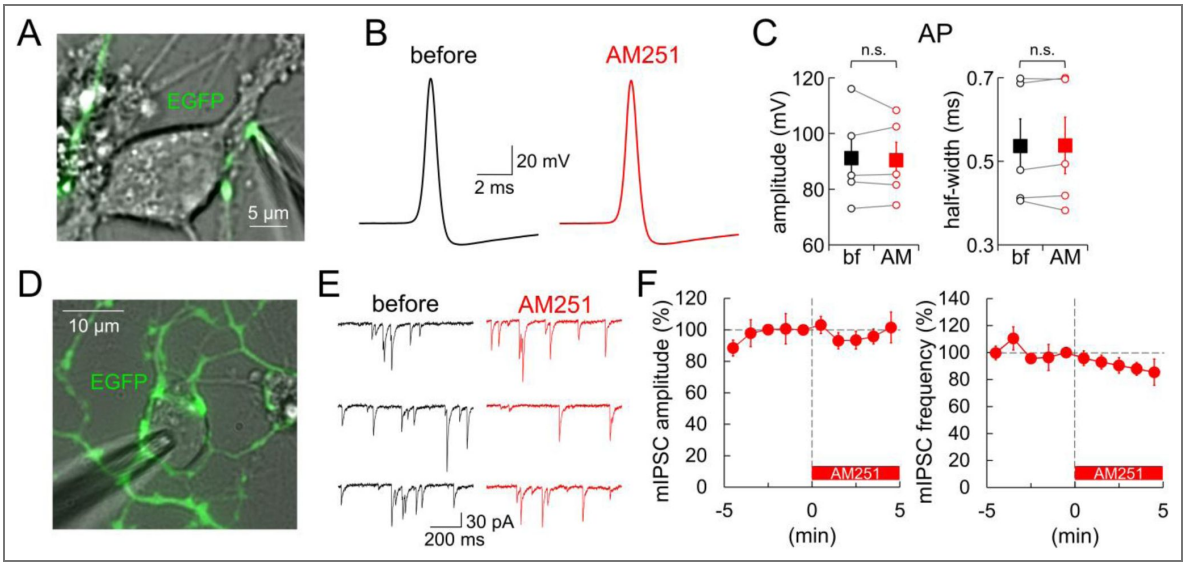

## GPR55 decreases the amount of vesicles in the readily-releasable pool

To obtain insights into the mechanism of GPR55-mediated suppression of neurotransmitter release, we biophysically analyzed the relation between presynaptic $Ca^{2+}$ influx and vesicle exocytosis by systematically changing depolarization pulses to a PC bouton. Depolarizing pulses with different length altered the duration of presynaptic $Ca^{2+}$ current, leading to distinct amounts of vesicular release (Figure 5A). As summarized in Figure 5B, the $Ca^{2+}$ current amplitude and its activation kinetics were again not significantly affected by GPR55 activation (amplitude, p = 0.424; tau, p = 0.339, ANOVA), supporting the idea that GPR55 does not affect the presynaptic $Ca^{2+}$ influx. On the other hand, $\Delta C_m$ induced by any duration of depolarization pulses showed ~50% reduction in the presence of AM251 (31 ± 6 fF/pF and 15 ± 2 fF/pF upon 50 ms pulse without and with AM251, respectively, p = 0.0289, Tukey-Kramer test) (Figure 5C, D). Thus, GPR55 halves the amount of synaptic vesicles released within tens of milliseconds after a strong $Ca^{2+}$ influx, corresponding to the readily-releasable pool (RRP), presumably consisting of immediately releasable and slowly releasable vesicles as in other boutons such as calyx of Held (Sakaba, 2006). The decrease of RRP vesicles could be the primary cause for the decrease in AP-triggered synaptic transmission. We also examined whether LPI, an endogenous agonist for GPR55, exerts a similar effect. When GPR55 was activated by LPI, $\Delta C_m$ was smaller in size (17 ± 2 fF/pF upon 50 ms pulse, p = 0.0488, compared with control, Tukey-Kramer test) to an extent of that by AM251, which was not enhanced by additional application of AM251 (16 ± 4 fF/pF upon 50 ms pulse, p = 1.00, compared with LPI alone, Tukey-Kramer test) (Figure 5—figure supplement 1). These results indicate that both LPI and AM251 act through GPR55 and reduce the RRP.

Taking into consideration that the cytoplasm of PCs contains extremely potent $Ca^{2+}$ buffering capacity due to the large amount of calbindin (Fierro and Llano, 1996; Bornschein et al., 2013), releasable vesicles in PC boutons might show steep dependency of their release competency on their position relative to the voltage-gated $Ca^{2+}$ channels (VGCCs). Previous studies reported that vesicular fusion is insensitive to exogenous EGTA in the intracellular solution, a relatively slow but high-affinity $Ca^{2+}$ buffer, suggesting that vesicles tightly coupled to VGCCs are release-competent in PC boutons (Kawaguchi and Sakaba, 2015; Diaz-Rojas et al., 2015). Indeed, the RRP size was comparable between 0.5 and 5 mM cytoplasmic EGTA conditions (0.5 mM EGTA, 30 ± 5 fF/pF; 5 mM EGTA, 34 ± 4 fF/pF upon 50 ms pulse, p = 0.928, Tukey-Kramer test) (Figure 5C and Figure 5—figure supplement 2). On the other hand, previous studies showed decrease in release by EGTA at synapses with relatively loose coupling between VGCCs and releasable vesicles, such as squid giant synapses, calyx of Held synapses, or hippocampal mossy fiber synapses (Adler et al., 1991; Borst and Sakmann, 1996; Vyleta and Jonas, 2014). Therefore, if GPR55 loosens the $Ca^{2+}$-release coupling, EGTA might become influential to the release even in PC boutons. However, the increase in cytoplasmic EGTA from 0.5 to 5 mM did not reduce the apparent RRP size in PC boutons when GPR55 was activated by AM251 (5 mM EGTA, 16 ± 3 fF/pF upon 50 ms pulse with AM251, p = 0.992, compared to 15 ± 2 fF/pF with 0.5 mM EGTA and AM251, Tukey-Kramer test) (Figure 5C). Notably, plotting the fold reduction of $\Delta C_m$ by AM251 against the duration of depolarization suggested that a higher amount of EGTA augmented the suppressive effect of GPR55, particularly for the release in response to short pulses (Figure 5D). This result implies that the reduction of release by GPR55 might be somehow related to the $Ca^{2+}$-release coupling, although its extent is too small to be reflected as a clear change of release sensitivity to EGTA. In summary, based on biophysical analysis of $Ca^{2+}$-dependent release in terms of the modulations by GPR55 and cytoplasmic EGTA, we conclude that the GPR55 activation reduces the amount of vesicles in the RRP, which might be accompanied by a slight change of the functional coupling between release and $Ca^{2+}$ influx.

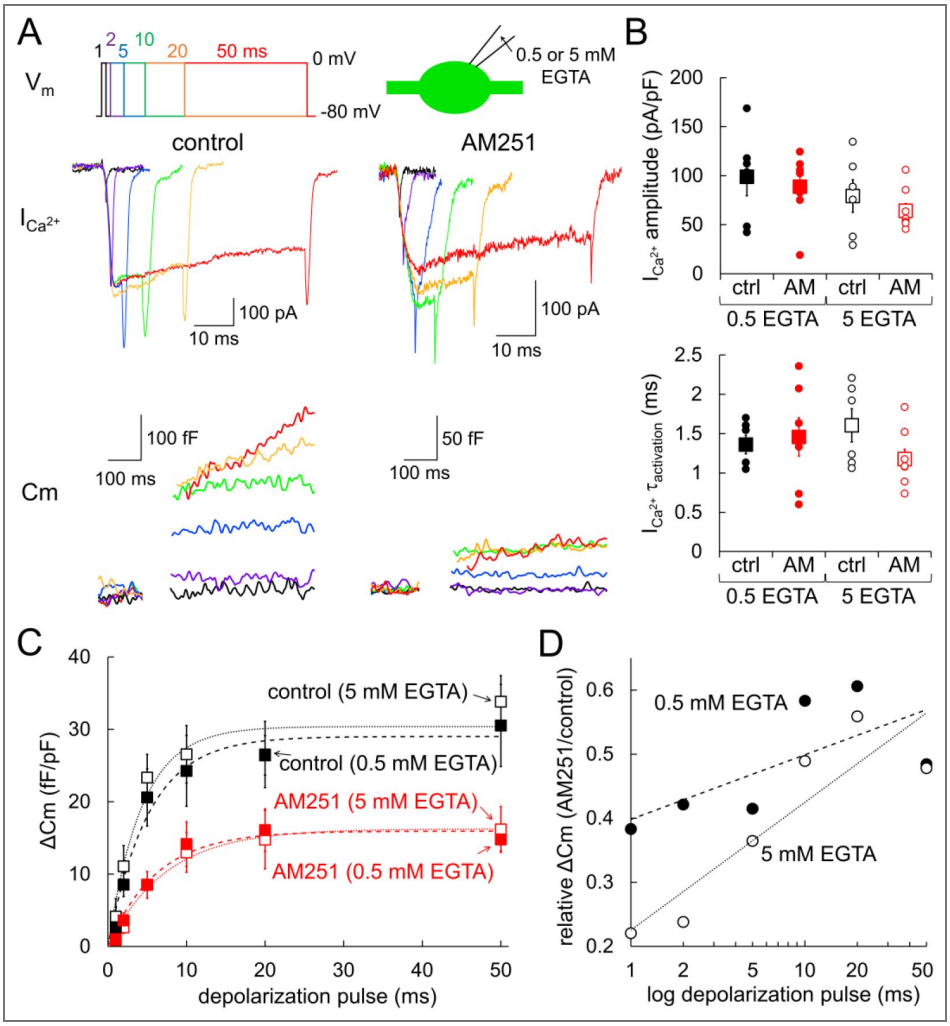


**Figure 5. Decrease in RRP vesicles by GPR55**

(**A**) Representative traces of presynaptic $I_{Ca2+}$ (middle) and the resultant $C_m$ increase (bottom) recorded with presynaptic 0.5 mM EGTA upon 1, 2, 5, 10, 20, or 50 ms of depolarization pulses (to 0 mV) (top) without (left) or with (right) AM251. Experiments were performed with a presynaptic patch pipette containing 0.5 mM or 5 mM EGTA. (**B**, **C**) Amplitude and time constant for activation of $I_{Ca2+}$ (B), and $C_m$ change (C) upon depolarization pulses recorded without (black, 0.5 mM EGTA, n = 6; 5 mM EGTA, n = 6) or with AM251 (red, 0.5 mM EGTA, n = 7; 5 mM EGTA, n = 8). Single exponential fits for each are shown as dotted lines. Both $I_{Ca2+}$ and $C_m$ change were normalized by the size of presynaptic $C_m$ under the voltage-clamp. In B, data for individual cells (circles) and mean ± SEM (squares) are shown. (**D**) Ratio of $C_m$ increase ($C_m$ increase with AM251 divided by that in control) recorded with 0.5 or 5 mM presynaptic EGTA is plotted against the logarithm of pulse duration.

## Slowed vesicular fusion by GPR55

To further investigate the GPR55-mediated downregulation of vesicular fusion, the $Ca^{2+}$-activated release kinetics were biophysically analyzed by simultaneous patch-clamp recordings from both a presynaptic PC bouton and a postsynaptic cell. To avoid saturation of postsynaptic $GABA_A$ receptors, we applied a short depolarization pulse (0 mV, 2 ms) to the patched bouton, and recorded presynaptic $Ca^{2+}$ and postsynaptic currents (Figure 6A). In line with the above results, presynaptic $Ca^{2+}$ current showed little change by the AM251 administration (42.1 ± 7.9 to 44.8 ± 9.9 pA/pF, p = 0.332, paired t-test), while postsynaptic currents were clearly reduced by half (2.57 ± 0.97 to 1.38 ± 0.63 nA, p = 0.0448, paired t-test) (Figure 6A, B). By deconvolving the postsynaptic currents with the template mIPSC trace, we estimated the temporal change of vesicular fusion velocity (for detail, see Methods; Kawaguchi and Sakaba, 2015). The peak of vesicular fusion velocity was almost halved by AM251 without a marked change of time course (45.7 ± 19.1 to 24.7 ± 11.3 vesicles/ms, p=0.0467, paired t-test) (Figure 6C), showing similar reduction to that observed in the apparent RRP size (vesicular fusion velocity: 46.9 ± 4.4%; $\Delta C_m$: 48.4% upon 50 ms pulse shown in Figure 5D). Thus, it would be reasonable to conclude that the RRP reduction, but not a change in the $Ca^{2+}$-activated release probability, predominantly underlies the synaptic suppression induced by GPR55. However, notably, AM251 induced a modest yet significant increase in synaptic delay, estimated by the time to the onset of release (onset of vesicular release: 1.63 ± 0.20 to 2.08 ± 0.33 ms, p = 0.0403, paired t-test) (Figure 6C). Thus, together with the idea that GPR55 somehow lowers the effectiveness of $Ca^{2+}$-triggered release (as shown in Figure 5D), the apparent RRP reduction by GPR55 in PC boutons might be caused by a process accompanied with a slight downregulation of the $Ca^{2+}$-mediated activation process of vesicular fusion.

## Reduction of AP-sensitive vesicles by GPR55

The above experiments demonstrated that GPR55 suppresses synaptic transmission primarily by reducing the RRP size without altering $Ca^{2+}$ influx at the presynaptic terminal. To discriminate two possible causes for the decrease in RRP size: relative increase in the fraction of reluctant vesicles or reduction of total vesicles present at the presynaptic terminal, we performed fluorescence imaging of vesicular fusion with synapto-pHluorin expressed in PCs using AAV or microinjection of plasmid DNA into the nucleus. First, APs were repetitively evoked (400 APs at 20 Hz) at the voltage-clamped PC soma by depolarization pulses triggering somatic $Na^+$ currents (Figure 7—figure supplement 1), and the fluorescence changes of pHluorin at axon terminals were monitored. Synapto-pHluorin shows little fluorescence upon light illumination when its pH-sensitive fluorophore is exposed to the acidic vesicular lumen, and becomes fluorescent after exocytosis through exposure to the external neutral pH environment (Figure 7A), providing the sign of vesicle fusion as a fluorescence increase (Sankaranarayanan and Ryan, 2000). As shown previously (Kawaguchi and Sakaba, 2015), PC axonal varicosities exhibited synapto-pHluorin fluorescence increase by 23.3 ± 2.0% upon 400 APs at 20 Hz (Figure 7B-D). After the increase in fluorescence during the AP train stimulation, pHluorin signal decayed with a time constant of about 40 sec, reflecting the endocytosis of exocytosed synapto-pHluorin and the subsequent re-acidification of the vesicular lumen (Nicholson-Tomishima and Ryan, 2004; Yamashita et al., 2018). In accord with the GPR55-mediated reduction of synaptic transmission (see Figure 1), AM251 administration reduced the pHluorin signal increase evoked by the 400 APs ($\Delta F_{400APs}$) by 53.8 ± 17.0% in average (p < 0.001, by paired t-test), with no change in its decay time course ($\tau_{decay}$: 42.1 ± 7.8 to 40.9 ± 4.5 sec, p = 0.780, paired t-test) (Figure 7C). The AP-triggered increase in pHluorin fluorescence was specific to axonal varicosities, and the GPR55 activation reduced the size of the fluorescence increase with substantial variability among individual boutons (Figure 7B-D). Altered abundance of GPR55 in distinct boutons might be responsible for the variable effect of AM251 (see Figure 2). Interestingly, however, plotting the extent of release reduction by AM251 against the original size of $\Delta F_{400APs}$ indicated that boutons showing a larger amount of release tend to be more susceptible to suppression by the GPR55 activation (Figure 7E). This indicates that the variable control of the synaptic output exerted by GPR55 depends on the original amount of release in individual boutons along a PC axon. On the other hand, when the

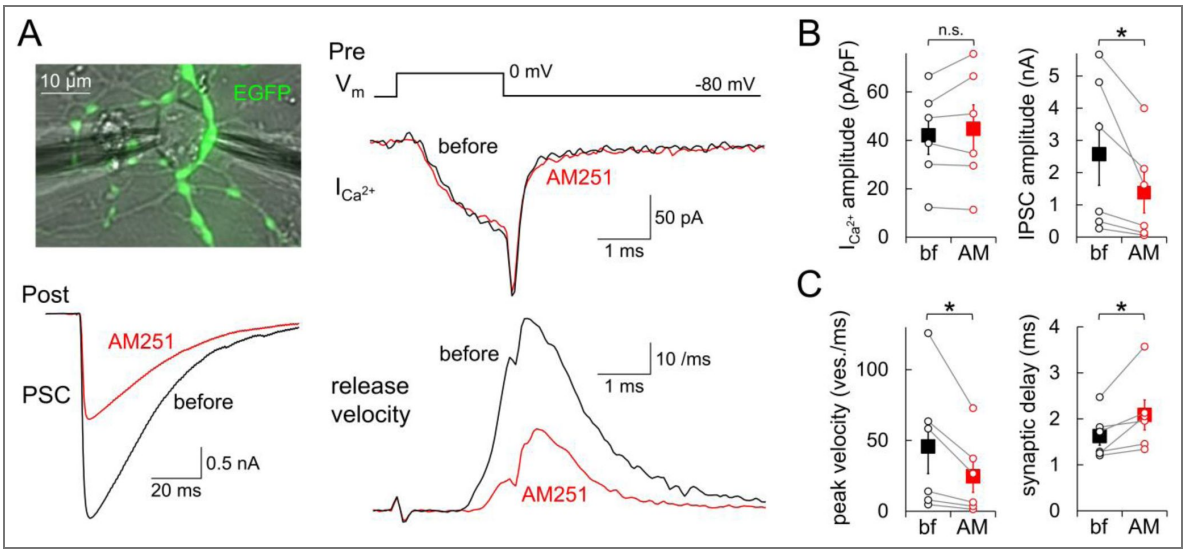


**Figure 6. Halved velocity of exocytosis shown by pre- and postsynaptic paired recordings**

(**A**) Image of paired recordings from a presynaptic EGFP-labeled PC bouton and its postsynaptic neuron (upper left), and representative traces of the presynaptic $I_{Ca2+}$ (upper right), IPSC (lower left), and velocity of vesicular fusion (bottom right; calculated by the deconvolution of IPSC trace) upon 2 ms depolarization before and after the AM251 application. (**B, C**) Amplitude of $ICa^{2+}$ (B, left, calibrated by the presynaptic $C_m$ under the voltage-clamp), IPSC (B, right), maximal release velocity (C, left) and synaptic delay (C, right) before and after application of AM251. The internal solution contained 0.5 mM EGTA. Data are mean ± SEM. * $p < 0.05$; n.s., not significant. n = 6 pairs.

intracellular vesicles with an acidic internal lumen were ubiquitously neutralized by exogenous application of $NH_4Cl$ (50 mM), as depicted in Figure 7A, pHluorin fluorescence increased by 356.8 ± 12.3% in the control condition and 352.3 ± 14.0% in the presence of AM251 (p = 0.811, Student's t-test) (Figure 7F, G), indicating that the total amount of vesicles at individual boutons is not affected by GPR55 activation. It should be noted that $\Delta F_{400APs}$ by itself exhibited a large variability across boutons, showing a linear relation to the 2/3rd power (for calibration between volume and surface area of boutons) of that by $NH_4Cl$ ($\Delta F_{NH4Cl}$) (Figure 7H). Thus, the fraction of releasable vesicles in response to APs seemed constant among distinct boutons: larger boutons containing more vesicles simply show higher $\Delta F_{400APs}$. In addition, the predicted distribution pattern of $\Delta F_{400APs}$ with GPR55 activation calculated from the relation between the extent of GPR55-mediated release reduction and the $\Delta F_{400APs}$ (shown in Figure 7E) nicely overlapped the actual data obtained after the AM251 application (Figure 7H). Thus, the fluorescent live imaging of AP-triggered vesicle fusion revealed that GPR55 reduces vesicular fusion in response to APs, without changing total vesicles present at individual PC boutons.

To obtain further insights into the dynamics of synaptic vesicular pools possibly affected by GPR55, such as transitions among the readily-releasable, recycling, reserve, and release-reluctant pools at individual boutons (Fernandez-Alfonso and Ryan, 2008; Kim and Ryan, 2010; Cazares et al., 2016; Mori et al., 2021), we repeatedly induced the 400 APs firing at the soma and measured the size of the fluorescence increase at boutons before and after the suppression of re-acidification of endocytosed vesicles with bafilomycin (100 nM), an inhibitor of vesicular ATPase (Sankaranarayanan and Ryan, 2001). As shown in Figure 8A (black trace), bafilomycin application enhanced the $\Delta F_{400APs}$ (by 55.9 ± 12.8%, p < 0.001, paired t-test), and abolished the fluorescence decay after the end of the stimulation (relative $\Delta F_{400APs}$ remaining at 40 sec after the end of APs: 59.8 ± 18.6 (control) to 97.6 ± 4.6% (bafilomycin), p = 0.0261, paired t-test), reflecting the inhibition of the re-acidification of endocytosed vesicles, which takes place in naïve conditions during and tens of seconds after the stimulation. Repeating the 400 APs stimulations after the bafilomycin application resulted in additive fluorescence increase, eventually reaching a plateau at 27.6 ± 2.6% of the maximal fluorescence increase observed after the $NH_4Cl$ application (Figure 8A). Imaging of presynaptic $Ca^{2+}$ increase with GCaMP7f expressed in PCs by AAV showed that $Ca^{2+}$ increase upon 400 APs remained constant during repetitive AP trains (Figure 8—figure supplement 1A, B). Thus, synaptic vesicles corresponding to those for ~1000 APs are totally release-competent at individual axon terminals, in accord with previous studies (Kawaguchi and Sakaba, 2015). In order to induce the exocytosis of the remaining releasable vesicles in the terminal, if any, after the 8 sets of 400 APs train stimulation, KCl (50 mM) was added to the external bath to potently depolarize the plasma membrane, resulting in widespread elevation of intracellular $Ca^{2+}$ (Figure 8—figure supplement 1). Nevertheless, little further increase in the pHluorin signal was observed upon KCl application (Figure 8A), confirming that most depolarization-sensitive vesicles have undergone fusion during the AP trains.

Intriguingly, the $\Delta F_{400APs}$ reduction by AM251 (red trace in Figure 8A) was evident throughout the 400 APs train stimulations (~10 minutes in total), reaching a plateau of about 13.2 ± 1.4% of the total amount of vesicles (Figure 8A, p < 0.001, compared with control (27.6 ± 2.6%), Student's t-test). This implies that the total releasable vesicles upon repeated APs for minutes, which are composed of the RRP, the recycling pool, and even some reserve pool of vesicles, get smaller in number when GPR55 is activated. To further obtain insight into the reduced releasable vesicles by GPR55, we triggered vesicular release from PC boutons by causing an aberrant cytoplasmic $Ca^{2+}$ increase by adding ionomycin, which forms $Ca^{2+}$-conducting pores on the plasma membrane. Indeed, when monitored by GCaMP7f fluorescence imaging, ionomycin (10 μM) induced a much more potent and broader $Ca^{2+}$ increase throughout PC axons than the $Ca^{2+}$ increase induced by the inflow through VGCCs upon APs stimulation (Figures 8C-E and Figure 8—figure supplement 1C; ΔF/F upon 400 APs and ionomycin: varicosity, 5.3 ± 0.4 and 16.2 ± 0.9, p < 0.001, Tukey-Kramer test; axon, 1.6 ± 0.2 and 15.1 ± 1.0, p < 0.001, respectively). Consequently, surprisingly, application of ionomycin increased pHluorin signal to almost identical levels irrespective of the GPR55 activation (54.0 ± 1.6% and 58.1 ± 3.9% of total vesicles without and with AM251, respectively, p = 0.356, Student's t-test) (Figure 8B). It should be noted that the size of the vesicle

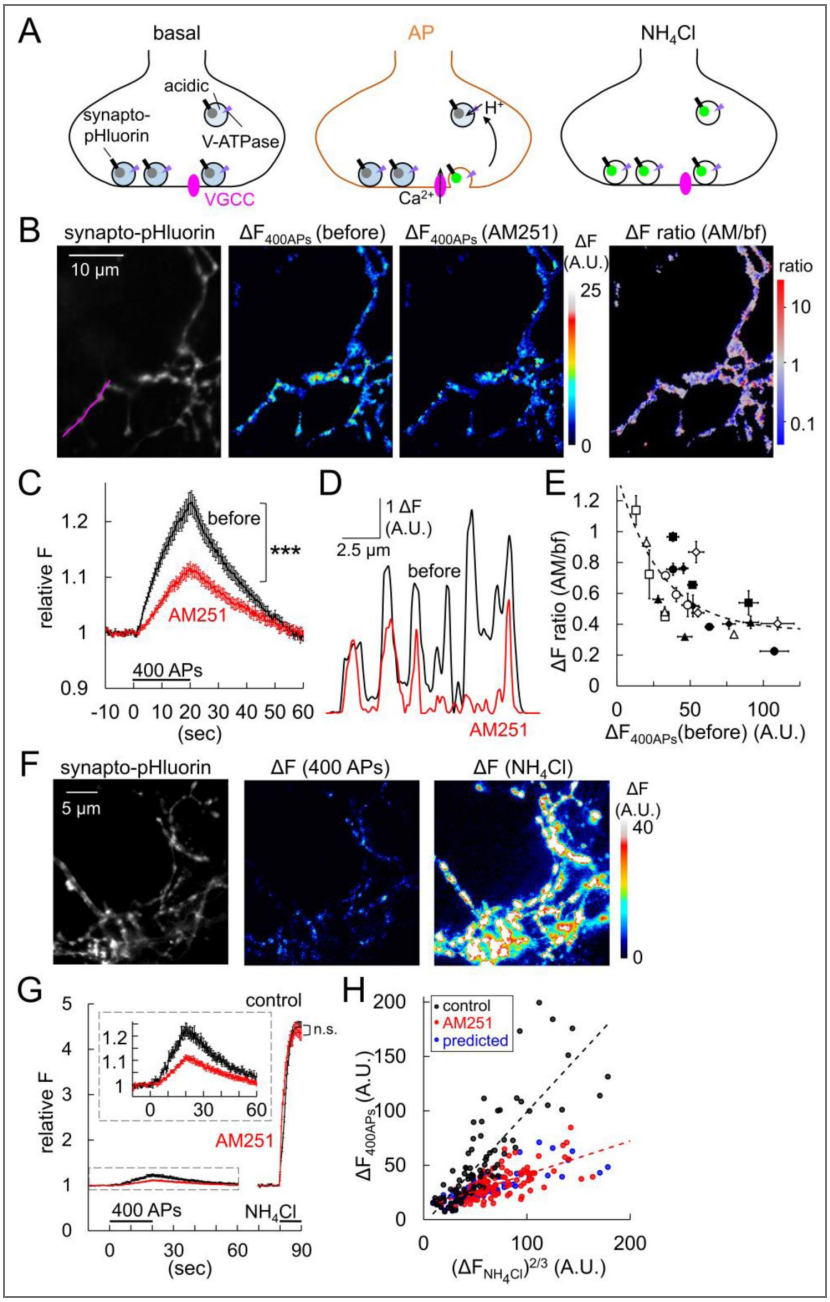


**Figure 7. Halved vesicular releases by GPR55 imaged with pHluorin**

(**A**) Schematic illustration for imaging of vesicle exocytosis with synapto-pHluorin. Upon vesicular fusion at the AP arrival, pHluorin becomes fluorescent because of exposure to the neutral pH. $NH_4^+$ application forcefully neutralizes vesicle lumen. (**B**) Representative images of synapto-pHluorin fluorescence and the color-coded fluorescence increase upon 400 APs ($\Delta F_{400APs}$) in PC terminals before and after the AM251 application. The right-most panel shows the ratio of fluorescence increase after the AM251 application relative to that before, represented in pseudo-color. (**C**) Time courses of 400 APs-triggered pHluorin fluorescence changes before and after the AM251 application. (**D**) Plot of $\Delta F_{400APs}$ along a PC axon (indicated as a magenta line in B) before and after the AM251 application. (**E**) Ratio of $\Delta F_{400APs}$ after the AM251 application relative to that before is plotted against the $\Delta F_{400Aps}$ before the AM251 application. Data from different cells are shown as different symbols. n = 8 cells. Dashed line represents data fitting with a function: $y = 1.02e^{-0.0334x} + 0.355$, $R^2 = 0.506$. (**F**) Images of pHluorin fluorescence and the color-coded fluorescence increases in a PC axon upon 400 APs and the following $NH_4Cl$ application (50 mM). (**G**) Time courses of synapto-pHluorin fluorescence changes upon 400 APs and the following $NH_4Cl$ application without or with AM251. Inset shows enlarged traces. (**H**) $\Delta F_{400APs}$ is plotted against the 2/3rd of ΔF caused by $NH_4Cl$ ($\Delta F_{NH4_{Cl}}$) for individual boutons without or with AM251. The effect of AM251 was predicted (blue) by conversion of dataset for control (black) based on the relationship shown in E, showing similar distribution to the actual data obtained with AM251 (red). Fitted line for control: $y = 1.03x - 4.05$, $R^2 = 0.704$; for AM251, $y = 0.307x + 10.9$, $R^2 = 0.441$. Data are mean ± SEM. *** $p < 0.001$; n.s., not significant.

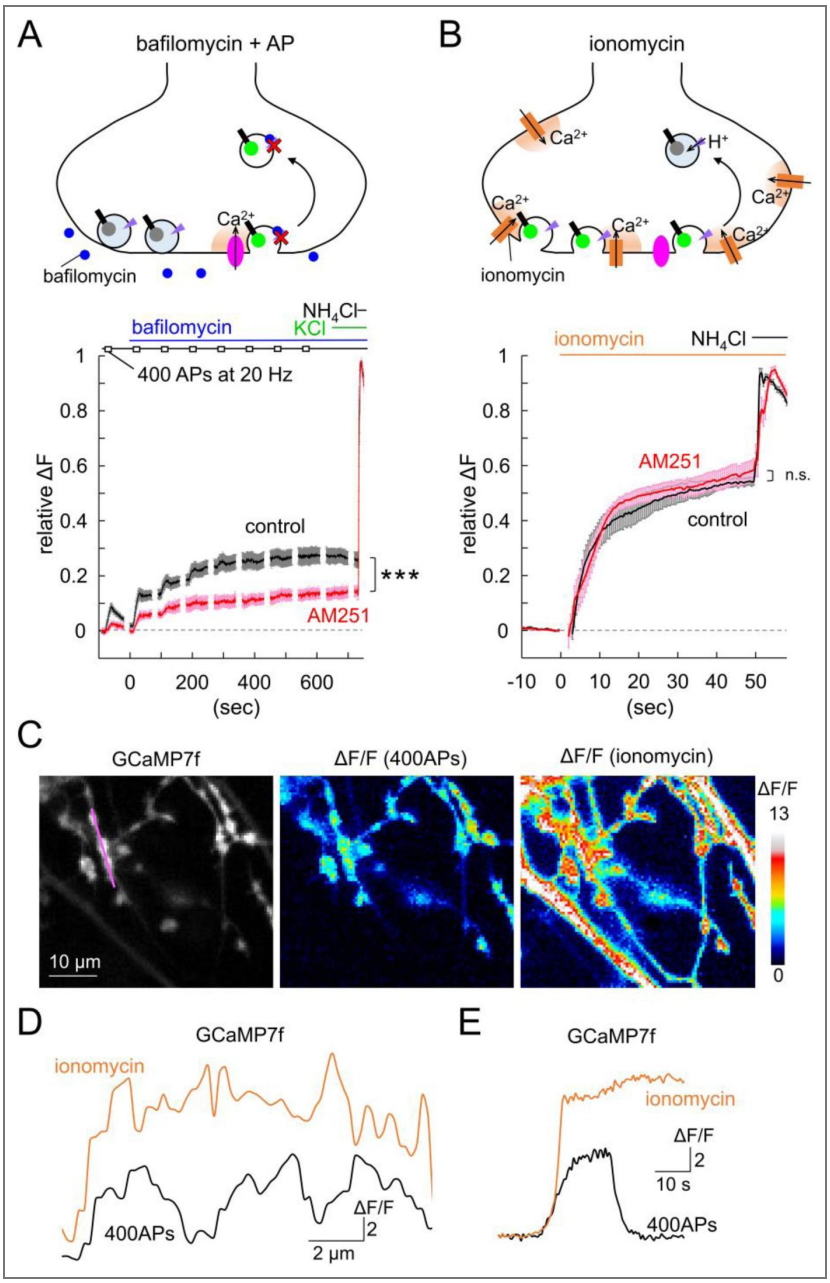


**Figure 8. Increase in reluctant vesicles insensitive to APs by GPR55**

(**A, B**) Schematic illustration (top) and time courses of synapto-pHluorin fluorescence changes at PC axon varicosities upon the repetitive 400 APs trains (20 Hz) before and after the application of bafilomycin and KCl (finally 50 mM) (A), or ionomycin (B), followed by the $NH_4Cl$ application, in the presence or absence of AM251. Data are mean ± SEM. *** $p < 0.001$; n.s., not significant. (**C**) Fluorescent images of GCaMP7f expressed in PC axon terminals (left) and color-coded relative fluorescence increase (ΔF/F) upon 400 APs at 20 Hz (middle) or the following ionomycin application (right). (**D, E**) Distribution patterns along an axonal segment (D; indicated as the magenta line in C) or representative time courses (E) of ΔF/F caused by 400 APs or ionomycin.

pool which underwent fusion upon the ionomycin application was almost double of the pool which underwent exocytosis upon thousands of APs. Thus, only a half population of $Ca^{2+}$-responsive releasable vesicles may be sensitive to APs in naïve PC axonal terminals, which is further reduced when GPR55 is activated.

# Discussion

In this study, we used a combination of subcellular patch-clamp recordings from axon terminals and fluorescence imaging of presynaptic vesicular exocytosis in cerebellar primary cultures, together with electrophysiology in cerebellar slices, and demonstrated that synaptic transmission from PCs is suppressed by activation of GPR55, a type of cannabinoid receptor. The mechanism of action involves a transformation of the presynaptic vesicles into insensitive to APs, while the $Ca^{2+}$ influx is kept constant in the terminal. Thus, a unique mechanism to negatively control synaptic outputs is unveiled here, which would provide a way to fine-tune the neuronal computation in the brain in coordination with the modulation of synaptic efficacy by conventional cannabinoid receptors.

## Modulation of synaptic function by endocannabinoids

Following the findings of critical roles of CB1 receptor in fine tuning of neuronal circuit function, another type of cannabinoid receptor, GPR55, was identified (Baker et al., 2006; Oka et al., 2007). GPR55 seems to be activated by 2-AG and anandamide, similarly to CB1 or cannabinoid receptor type 2 (CB2), although the downstream signaling is different, and also shows affinity to cannabidiol, another molecule found in cannabis (Henstridge et al., 2008; Oka et al., 2009). Distinct from typical chemical components of cannabis such as tetrahydrocannabinol (THC), cannabidiol has been shown to modulate the function of nervous system with limited addictive power, and thus has attracted attention for possible therapeutic applications to mental disorders (Denis et al., 2024). Thus, the physiological actions of GPR55 are now increasingly studied, although its detailed effect on neuronal computation still remains largely veiled. Here, we observed a remarkable suppression of presynaptic function by GPR55 in PC boutons through a change in the releasable vesicle amounts and/or properties. Pioneering studies clarified an important role of GPR55 in synaptic transmission at hippocampal excitatory synapses, demonstrating presynaptic enhancement of glutamate release presumably by elevating the cytoplasmic residual $Ca^{2+}$ via release from intracellular stores (Sylantyev et al., 2013; Rosenberg et al., 2023), in contrast to the suppression of release in our observation. The lack of positive modulation of AP-triggered release through residual $Ca^{2+}$ in PC terminals might be due to abundant amount of potent $Ca^{2+}$ buffer calbindin (Fierro and Llano, 1996). Indeed, increased vesicular fusion only for the AP-insensitive spontaneous vesicular release (as mIPSCs) was observed upon the $IP_3$-mediated $Ca^{2+}$ release from internal store (Gomez et al., 2020). Thus, minimal sensitivity of AP-triggered release to residual $Ca^{2+}$ in PC boutons would underlie the distinct effects of GPR55 activation at the presynaptic side. In addition, Rosenberg et al. (2023) also demonstrated postsynaptic modulation by GPR55 at hippocampal inhibitory synapses: reduction of postsynaptic $GABA_A$ receptors whereas limited presynaptic expression of GPR55 at axons. Here we showed clear GPR55 signals at PC terminals (see Figure 2), whereas no detectable changes in mIPSC amplitudes were observed upon GPR55 activation in potential DCN neurons (see Figure 4E, F). Thus, distinct combination of critical factors, such as amount and/or location of GPR55 expression, subtypes of postsynaptic $GABA_A$ receptors, and/or their anchoring mechanism, might give rise to various forms of modulation of synaptic strength by GPR55, as demonstrated in the hippocampus and cerebellum.

One extensively studied activity-dependent short-term depression of synaptic strength in the CNS is DSE and/or DSI, which are typically caused by a strong postsynaptic depolarization accompanied with potent $Ca^{2+}$ increases or activation of $G_q$-coupled metabotropic receptors such as group-I mGluRs, activating PLC and/or diacylglycerol lipase. Both enzymes produce typical endocannabinoids such as 2-AG and anandamide, which then reach retrogradely presynaptic boutons beyond plasma membranes and synaptic cleft (Kano et al., 2009; Castillo et al., 2012).

As a result, CB1 receptor located at the presynaptic membrane is activated and then $Ca^{2+}$-triggered transmitter release is suppressed for tens of seconds (Kreitzer and Regehr, 2001; Ohno-Shosaku et al., 2001; Wilson and Nicoll, 2001; Diana et al., 2002). Such short-term forms of presynaptic plasticity have been found to take place at a variety of synapses in the CNS including the hippocampus, cerebellum, prefrontal cortex, amygdala, and so on (Kano et al., 2009; Di Marzo et al., 2001; Katona 2001; Hill and Patel, 2013), which has provided basic knowledge about the primary mechanisms of cannabis intake affecting brain computation. In addition, CB1 receptor has been shown to play roles in long-term synaptic plasticity and hence learning and memory in animals (Kano et al., 2009; Gómez-Gonzalo et al., 2015). On the other hand, the functional role of another cannabinoid receptor CB2 has been largely unknown. CB2 receptor exogenously expressed in hippocampal autaptic neurons from CB1 null mice was shown to suppress synaptic transmission and restore DSE (Atwood et al., 2012). In contrast, in spite of CB2 being expressed in PCs (Ashton et al., 2006), no modulation of synaptic outputs from PC axons has been demonstrated (Hirono and Yanagawa, 2021). Thus, as demonstrated here, PC axon terminals might be equipped with a compensatory mechanism to control outputs through GPR55 in place of CB2 receptor.

## Mechanisms for synaptic modulations by GPR55 distinct from CB1/CB2 receptors

Unlike typical metabotropic receptors, here we have shown that GPR55 reduces vesicular exocytosis by converting the $Ca^{2+}$-sensitive release-competent vesicles into reluctant ones upon AP arrival, without changing the $Ca^{2+}$ influx and vesicular $Ca^{2+}$ responsiveness (see Figure 3-8). Rapid replenishment and/or endocytosis of synaptic vesicles are known to depend on actin dynamics (Lee et al., 2012; Miki et al., 2016), which might be related to the altered vesicular sensitivity to $Ca^{2+}$ influx through VGCCs after the GPR55 activation. In any case, the unique control of presynaptic function by $G\alpha_{12/13}$-coupled GPR55 demonstrated here would provide a complementary modulation of synaptic outputs by cannabinoids together with CB1/CB2 receptors. Previous studies have clarified the molecular mechanisms by which CB1 receptor negatively modulates synaptic transmission. As well as a typical inhibitory modulation by metabotropic receptors such as group-II metabotropic glutamate receptors and $GABA_B$ receptors (Kew et al., 2001; Takahashi et al., 1998; Bowery et al., 2002), CB1 and CB2 receptors are thought to couple to $G_{i/o}$-type trimeric G-protein, negatively regulating the activation and/or conductance of VGCCs (Guo and Ikeda, 2004). Taking it into consideration that the vesicular exocytosis steeply depends on the local $Ca^{2+}$ concentration around the $Ca^{2+}$ sensor, synaptotagmin (Schneggenburger and Neher, 2000), the reduction of $Ca^{2+}$ influx is enough to explain the suppression of transmitter release. Interestingly, when activated for minutes in cerebellar granule cells, CB1 receptor was also shown to downregulate the release competence of vesicles through their displacement from active zone (Ramírez-Franco et al., 2014), which is reminiscent of the GPR55-mediated RRP reduction we presented in this study. It would be interesting to highlight the difference in mechanisms how distinct G-protein cascades modulate the release machinery in the future study.

## Dynamics of synaptic vesicles among distinct functional pools

Inspired by the GPR55-mediated marked decrease in RRP vesicles demonstrated here by the presynaptic $C_m$ measurement and biophysical analysis, we live-imaged vesicular fusion with synapto-pHluorin to functionally dissect the altered pools of vesicles in PC terminals (see Figures 7, 8). Surprisingly, the reduction of release upon GPR55 activation was only evident when the release was triggered by APs, but undetectable in response to ionomycin, indicating that the apparent RRP reduction would be highly related to the source of cytoplasmic $Ca^{2+}$ increase. Taking into consideration that the RRP reduction was also evident when the $Ca^{2+}$ increase was triggered by much stronger stimulation (50 ms direct presynaptic depolarization or extracellular KCl application), the discrepancy between the effects of GPR55 on release by the presynaptic depolarization and the $Ca^{2+}$ ionophore could be reasonably ascribed to the relationship between

release sites and $Ca^{2+}$ sources. Alternatively, slower kinetics and more prolonged duration, in addition to higher amplitude, of $Ca^{2+}$ elevation upon ionomycin might somehow have resulted in more efficient trigger of exocytosis. Notably, our imaging experiments indicated that the total recycling pool of vesicles which underwent exocytosis by thousands of APs during ~10 minutes corresponds to only ~25% of total vesicles, that is, a half of $Ca^{2+}$-sensitive release-competent vesicles that could fuse upon aberrant $Ca^{2+}$ increase via the $Ca^{2+}$-conducting ionophore (see Figure 8A, B). Because of the extremely potent and rapid $Ca^{2+}$ buffering system in the cytoplasm of PCs due to the abundant expression of calbindin (Fierro and Llano, 1996), the $Ca^{2+}$ influx from VGCCs is expected to activate vesicles with the $Ca^{2+}$ sensor very close to the VGCCs. Thus, it is implied that the release-competent vesicles relatively far from VGCCs tend to stay at their position for minutes without being exocytosed or getting into the AP-sensitive pools. Indeed, it was shown that the relatively large increase in the cytoplasmic $Ca^{2+}$ concentration by $IP_3$-caused release from the internal $Ca^{2+}$ store in PC terminals, is only effective for the AP-independent spontaneous vesicular releases detected as miniature postsynaptic responses (Gomez et al., 2020). Thus, at least in PCs, the functional categorization of depolarization-sensitive vesicles seems to be influenced by the physical distance of vesicles and the source of $Ca^{2+}$. Interestingly, the reduction of releasable vesicles by GPR55 activation is limited to the AP-sensitive ones among $Ca^{2+}$-sensitive ones (see Figure 8). Taking the two findings together into consideration that GPR55 suppresses more potently the release caused by smaller $Ca^{2+}$ increase in the presence of high EGTA (see Figure 5) and delays the onset of release (see Figure 6), it would be reasonable to presume that the functional coupling between VGCCs and release machinery is loosened by the GPR55 activation. The loosened $Ca^{2+}$-release coupling, if any, upon GPR55 activation operating as the mechanism for synaptic suppression would compromise with the lack of changes in frequency of mIPSCs (see Figure 4B, C). The fact that GPR55 activation leads to altered actin cytoskeleton organization also makes this scenario plausible. Alternatively, it is also conceivable that GPR55 rather decreases the $Ca^{2+}$-dependent vesicle replenishment (Hosoi et al., 2007), which possibly leads to lower occupancy of release sites with release-competent vesicles, resulting in smaller total exocytic events in response to long depolarization (like that for 50 ms). This scenario would compromise with the tendency of more potent suppression of release by GPR55 with stronger $Ca^{2+}$ buffering by higher EGTA (see Figure 5D). On the other hand, it would also be possible that GPR55 somehow drives immature vesicles to the release sites, such as those immediately after endocytosed from the plasma membrane (Tran et al., 2023), leading to apparent reduction of transmitter release. Recent direct patch-clamp recordings combined with super-resolution fluorescence or electron microscopic imaging are highlighting the dynamic change of the $Ca^{2+}$-release coupling distance and/or efficacy (Fukaya et al., 2021; Midorikawa et al., 2024). The exact change of release machinery relative to VGCCs at high resolution of ~ nm in PC boutons upon GPR55 activation is a critical issue to be clarified in the future.

## Issues remain to be clarified in GPR55-mediated synaptic modulation

There are important issues to be unveiled in the future, as clarified for CB1 receptor: what neuronal situation leads to the production of endogenous GPR55 ligands like LPI, and how are the synapses modulated in terms of strength and time course? Multiple isoforms of LPI are known to have different chain length and unsaturation level, leading to distinct influence on GPR55 (Brenneman et al., 2025). The soy-derived LPI (obtained from Merck #L7635) which we used in this study, contains ~58% C16:0 and ~42% C18:0 or C18:2, and is known to exert neuroprotective and anti-inflammatory effects in cultured DRG neurons (Brenneman et al., 2025), together with just a little of the C20:4 isoform promoting neuroinflammatory action. Intracellular $Ca^{2+}$ elevation, such as pharmacologically caused seizures, leads to the LPI production at various CNS regions including the hippocampus (Yamashita et al., 2010; Rosenberg et al., 2023), although little is known about LPI in the cerebellum. Expression of LPI-producing phospholipase A1 and A2 in PCs (Shirai and Ito, 2004) would be a clue to study this issue.

In spite of the labeling of PC boutons with a fluorescent analogue of AM251 dependent on GPR55 gene expression (see Figure 2), direct evidence of specific localization of GPR55 at PC boutons, for example by immuno-labeling, is missing at present due to the unavailability of a qualified and specific antibody as far as we have tested. Further, the present study could not identify the downstream mechanism how GPR55 deprives the release competent vesicles of sensitivity to APs. GPR55-coupled $G\alpha_{12/13}$–RhoA–actin pathway is expected to underlie, and detailed biophysical analysis in the future would answer which of $Ca^{2+}$-release coupling or $Ca^{2+}$-dependent vesicle replenishment is a likely candidate.

# Materials and Methods

## Animal usage

All experimental procedures were performed in accordance with regulations on animal experimentation in Kyoto University and approved by the local committee in Graduate School of Science, Kyoto University. Wistar rats (Slc: Wistar; Japan Slc Inc., Hamamatsu, Japan) of either sex were used in this study. Rats were housed with a mother rat until weaning in filter-top cages with bedding at 20–24°C under a 12/12 h light/dark photocycle. Food and water were available *ad libitum*. Rats were killed by decapitation, and older ones by anaesthetization with isoflurane in air, then decapitation.

## Slice preparation

Acute sagittal slices (200 μm thickness) of cerebellum were prepared from Wistar rats at P28-42. Rats were anesthetized with isoflurane and perfused transcardially with ice-cold sucrose solution containing the following (in mM): NaCl 60, sucrose 120, $NaHCO_3$ 25, $NaH_2PO_4$ 1.25, KCl 2.5, D-glucose 25, ascorbic acid 0.4, myo-inositol 3, Na-pyruvate 2, $CaCl_2$ 0.1, $MgCl_2$ 3, pH 7.3-7.4, 300-350 mOsm/kg $H_2O$ with continuous bubbling with mixed gas (95% $O_2$ and 5% $CO_2$). After decapitation, the cerebellum was quickly removed and cut with a Leica vibroslicer (VT1200S) in an ice-cold K-Gluconate-based solution containing the following (in mM): K-Gluconate 130, KCl 15, EGTA (ethylene glycol-bis(β-aminoethyl ether)-N,N,N',N'-tetraacetic acid) 0.05, HEPES (4-(2-hydroxyethyl)-1-piperazineethanesulfonic acid) 20, glucose 25, and D-AP5 50 μM, pH 7.4, 300-350 mOsm/kg $H_2O$, with continuous bubbling with mixed gas (95% $O_2$ and 5% $CO_2$). Slices were then incubated at 37 °C for a half to 1 h in an extracellular solution containing the following (in mM): NaCl 125, $NaHCO_3$ 25, $NaH_2PO_4$ 1.25, KCl 2.5, D-glucose 25, ascorbic acid 0.4, myo-inositol 3, Na-pyruvate 2, $CaCl_2$ 2, $MgCl_2$ 1, pH 7.3-7.4, 300-320 mOsm/kg $H_2O$ with continuous bubbling with mixed gas.

## Cerebellar primary cultures

The method for preparing primary dissociated cultures of cerebellar neurons was similar to that in previous studies (Kawaguchi and Hirano, 2007). Briefly, cerebella were dissected out from newborn rats and their meninges were removed. The cerebella were incubated in $Ca^{2+}$ and $Mg^{2+}$-free Hank's balanced salt solution containing 0.1% trypsin and 0.05% DNase for 15 min at 37°C. Cells were dissociated by trituration and seeded in Dulbecco's modified Eagle's medium: nutrient mixture F12-based medium containing 2% fetal bovine serum. On the next day, ~ 80% of medium was replaced by basal medium Eagle. After that, half of the medium was changed every 3–4 days. Cytosine arabinoside (4 μM) was added to the medium to inhibit proliferation of glial cells. PCs could be visually identified by large cell bodies and thick dendrites. Experiments were performed >21 days after preparation of the culture.

## DNA construction and transfection

Plasmids containing coding DNA sequences of synapto-pHluorin, EGFP, Venus, and GCaMP7f were the same as previous studies (Kawaguchi and Hirano, 2007; Kawaguchi and Sakaba, 2015; Higashi et al., 2024). DNA fragments for tTA and TRE sequences were obtained from Tet-Off system (Clontech). cDNAs were inserted into the pAAV-CA-WPRE plasmid (Higashi et al., 2024).

PCs were transfected with an AAV vector serotype 2 at 4-7 days after seeding. For GPR55-KD, the S. pyogenes Cas9 vector plasmid, pSpCas9(BB)-2A-miRFP670 was obtained from Addgene (#91854). Two gRNAs specific to GPR55 were designed with the CHOPCHOP online software. The target sequences were designed to be separated by 81 base pairs so that the extracellular domain for AM251 binding would be deleted (Joberty et al., 2020). The target sequences were cloned into the plasmid based on the published protocol by Ran et al., 2013. Briefly, pSpCas9(BB)-2A-miRFP670 was digested with BbsI (New England Biolabs, USA) and the following oligos, 5'-CACCGC CCCTGTGGAAAGTGTAGAT-3' and 5'-AAACATCTACACTTTCCACAGGGGC-3', or 5'-CACCGTGCGAGAGT CTTCTTCCCCC-3' and 5'-AAACGGGGGAAGAAGACTCTCGCAC-3' (Eurofins Genomics, Japan), were annealed and ligated into the digested plasmid. For GPR55-KD using CRISPR/Cas9 or some imaging experiments using synapto-pHluorin, the DNA expression plasmids encoding Cas9 and gRNAs, or synapto-pHluorin were directly injected into the nucleus of PCs through sharp glass pipettes (Kawaguchi and Hirano, 2007). Recordings from DNA-injected cells were performed 1–2 days after the injection, except for GPR55-KD cells with CRISPR/Cas9-mediated acute genome editing (at 5 days).

## Electrophysiology

Patch-clamp recording was performed with an amplifier (EPC10, HEKA Elektronik, Germany) at room temperature (20-24 °C), in an extracellular solution mentioned above for slices, or that containing the following for culture (in mM): NaCl 145, HEPES 10, glucose 10, $CaCl_2$ 2, $MgCl_2$ 1, pH 7.3-7.4 adjusted with KOH, and 300-310 mOsm/kg $H_2O$, using an inverted IX71 microscope (Olympus, Tokyo, Japan) equipped with a 40×, 0.95 numerical aperture (NA) objective or an upright BX51WI (Olympus) equipped with a 60×, 1.0 NA objective. Images were obtained with a Zyla4.2 sCMOS camera (Andor; Oxford Instruments, Oxford, UK). In some experiments, 2,3-Dioxo-6-nitro-1,2,3,4-tetrahydrobenzo[f]quinoxaline-7-sulfonamide (NBQX, 10 μM), tetrodotoxin (TTX, 1 μM) and tetraethylammonium (TEA, 2 mM) were applied to the bath. For current-clamp recordings, KCl-based internal solution with the following composition (in mM) was used: KCl 147, HEPES 10, EGTA 0.5, Mg-ATP 2, Na-GTP 0.2, pH 7.3-7.4 adjusted with KOH, and 320-330 mOsm/kg $H_2O$. For voltage-clamp recordings from PC-target neurons, a patch pipette was filled with a CsCl-based internal solution (pH 7.3-7.4 adjusted with CsOH and 320-330 mOsm/kg $H_2O$) containing (in mM): CsCl 147, HEPES 10, EGTA 0.5, Mg-ATP 2, Na-GTP 0.2. For voltage-clamp recordings from PC axon terminals, the internal solution was composed of (in mM): CsCl 103, KCl 44, HEPES 10, EGTA 0.5, Mg-ATP 2, Na-GTP 0.2 (pH 7.3-7.4 adjusted with CsOH and 320-330 mOsm/kg $H_2O$). In a subset of experiments shown in Figure 5, the EGTA concentration was increased to 5 mM. Presynaptic terminal recordings were performed in the presence of external TTX (1 μM) and TEA (2 mM). AM251 (5 μM for slice or 500 nM for culture; $EC_{50}$ = 39 nM, Ryberg et al., 2007), LPI (1 μM; $EC_{50}$ = 30 nM, Oka et al., 2007), or CID16020046 (5 μM; $IC_{50}$ = 0.21 μM, Kargl et al., 2013) were applied to the bath. LPI derived from soy (Merck, catalog #L7635) that was estimated to contain 58% C16:0 and 42% C18:0 or C18:2 was applied to the bath. Membrane potential of a PC was held at -70 mV unless otherwise stated. PCs' target postsynaptic neurons were voltage clamped at -70 to -100 mV (to avoid unclamped $Na^+$ currents) in slices, or at -70 mV in culture for IPSC recordings. Series resistance in recordings from the PC soma and axon terminal was online-compensated by 30−60%. For IPSC measurements, the remaining resistance was corrected off-line after the recording. In paired whole-cell recordings from a presynaptic PC soma and its postsynaptic neuron, APs were elicited by voltage pulses to 0 mV for 1-5 ms into PC soma. In the slice, IPSCs were evoked by a glass pipette placed in the white matter. The deconvolution analysis was performed as in a previous study (Kawaguchi and Sakaba, 2015) using a template of mIPSC waveform. The onset of release was defined as the first time point at which the calculated vesicular fusion velocity showed change larger than 2 SDs of that at the basal condition. Average amplitude and frequency of mIPSCs for individual cells were calculated from ≥ 200 events showing amplitude (≥ 7 pA) and appropriate time course.

Measurement of $C_m$ was done using sine + DC technique (Neher and Marty, 1982) implemented on the PatchMaster software (HEKA Elektronik, Germany). Presynaptic terminals were held at -80 mV and the sine wave (1 kHz and the peak amplitude of 30 mV) was applied on the holding

potential. Because membrane conductance fluctuates during the depolarizing pulse, $C_m$ was usually measured approximately 50 ms after the depolarization. To estimate the clamped area in a direct bouton recording, capacitive transients in response to a hyperpolarizing pulse (5 or 10 mV) were used. To normalize the variation in $Ca^{2+}$ currents and neurotransmitter release depending on the size of the bouton, presynaptic $Ca^{2+}$ current and $C_m$ were normalized by the $C_m$ under the voltage-clamp in each bouton (in Figure 3-6).

## Fluorescence imaging

For GPR55 fluorescent labeling, cultured neurons were incubated with T1117 (20 nM) in extracellular solution for 2 min at room temperature. Following incubation, cells were washed once with fresh extracellular solution to remove unbound dye and immediately imaged with a confocal fluorescence imaging system FV1000 (Olympus) using a 60× 0.9-NA water-immersion objective (Olympus) equipped on an upright microscope BX61WI. Fluorescence imaging of pHluorin or GCaMP7f was performed using an upright microscope BX51WI (Olympus) through a 60× 1.0-NA objective

(Olympus). Fluorescent excitation was delivered using an LED (M470L4, Thorlabs). Images of pHluorin or GCaMP7f fluorescence in PC axon terminals were obtained at 0.5 Hz with Zyla4.2 sCMOS camera (Andor), and analyzed with SOLIS (Andor) or ImageJ (NIH). APs were evoked at the voltage-clamped PC soma by depolarizing pulses (0 mV, 5 ms). Bafilomycin (100 nM), ionomycin (10 µM), KCl (50 mM), and $NH_4Cl$ (50 mM) were applied to the bath.

## Statistics

Data are presented as mean ± SEM unless otherwise stated. Statistical significance was evaluated by paired t-test, unpaired Student's t-test for unpaired groups, one-way ANOVA, Dunnett's test or Tukey-Kramer test for multiple comparisons. Statistical significance was defined as $p < 0.05$.

# Figure supplements

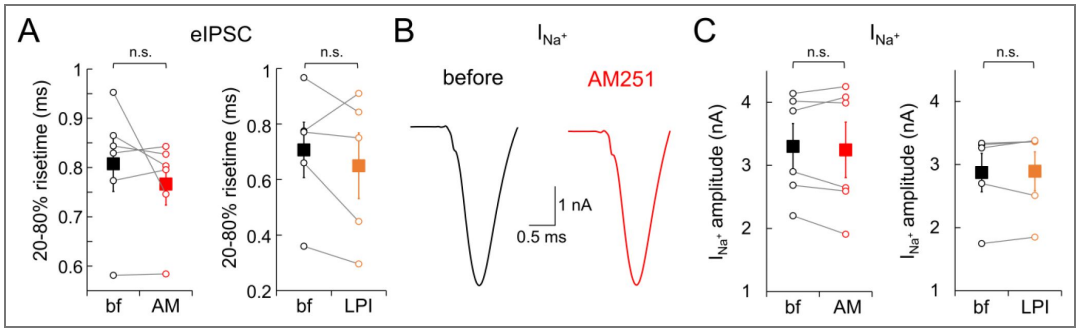


**Figure 1—figure supplement 1. No effects of GPR55 on IPSCs time courses and somatic $Na^+$ currents** (**A**) 20-80% risetime of eIPSCs before and after application of AM251 or LPI. Data for individual cells are also shown (open circles). (**B, C**) Representative traces (B) and amplitudes (C) of $Na^+$ current before and after application of AM251 or LPI. AM251, n = 6; LPI, n = 5. Data are mean ± SEM. n.s., not significant.

**Figure 4—figure supplement 1. No effects of GPR55 on time courses of mIPSCs**

20-80% risetime or half-width of mIPSCs before and after application of AM251 (n = 5). Data for individual cells are also shown (open circles). Data are mean ± SEM. n.s., not significant.

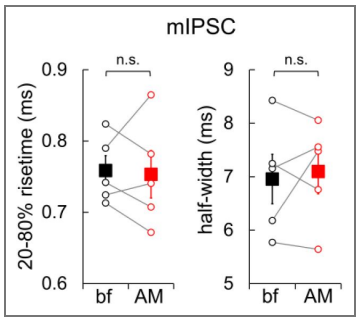


**Figure 5—figure supplement 1. AM251 and LPI occlude the suppressive effects on vesicle release each other**

(**A**, **B**) Amplitudes and time constants for activation of presynaptic $I_{Ca2+}$ (A), and $C_m$ changes (B) upon depolarization pulses recorded with LPI only (orange, n = 6) or with LPI and AM251 (purple, n = 6). For comparison, control and AM251 data (shown in Figure 5) are also presented. Single exponential fits for each are shown as dotted or solid lines. Both $I_{Ca2+}$ and $C_m$ change were normalized by the size of presynaptic $C_m$ under the voltage-clamp. In A, data for individual cells (open circles) and mean ± SEM (squares) are shown. The presynaptic internal solution contained 0.5 mM EGTA.

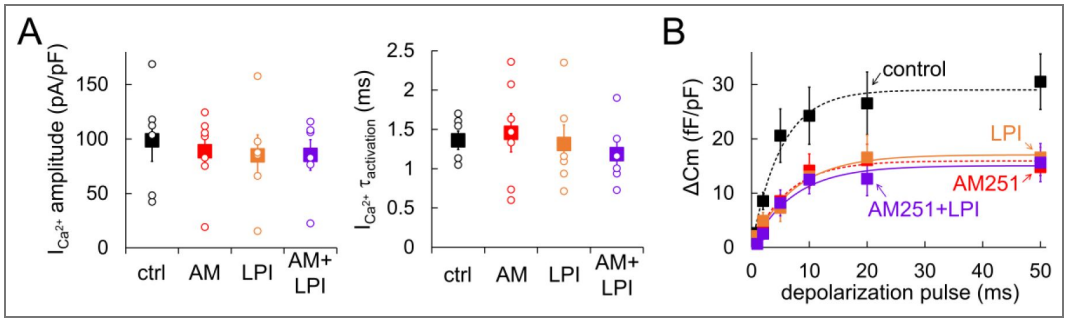

**Figure 5—figure supplement 2. GPR55-mediated suppression of release in PC boutons with 5 mM EGTA**

Representative traces of presynaptic $I_{Ca2+}$ (middle) upon 1, 2, 5, 10, 20 and 50 ms of depolarization (to 0 mV, depicted on the top) of a PC bouton, and the resultant $C_m$ increase (bottom) in the presence or absence of AM251. Recording was performed with a patch pipette containing 5 mM EGTA.

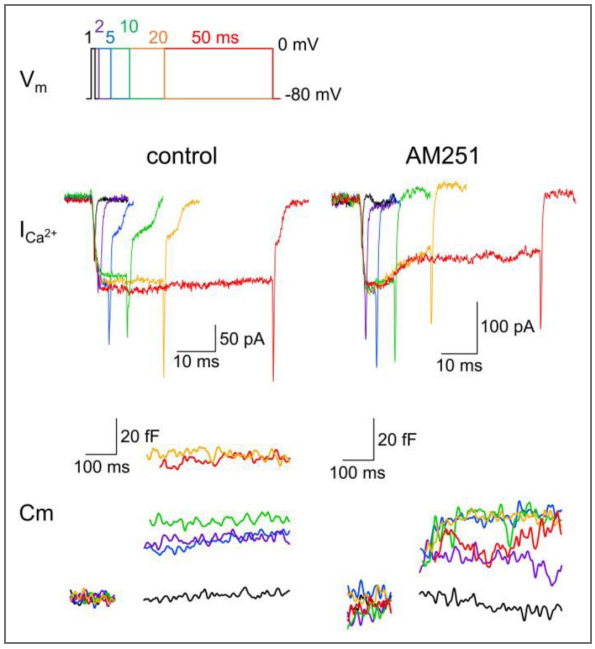


**Figure 7—figure supplement 1. No effects of GPR55 on somatic $Na^+$ currents upon repetitive stimulation at 20 Hz**

(**A**) Representative traces of $Na^+$ and $K^+$ currents before and after application of AM251. (**B**) Amplitudes of $Na^+$ current upon repetitive stimulation at 20 Hz before and after application of AM251 (n = 7). Data for individual cells are also shown (open circles). Data are mean ± SEM. n.s., not significant.

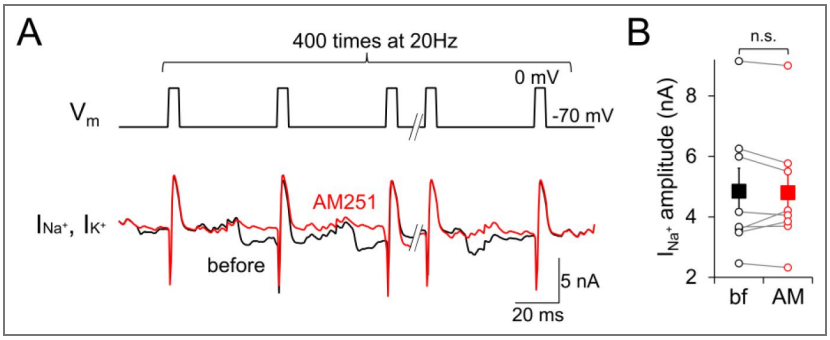

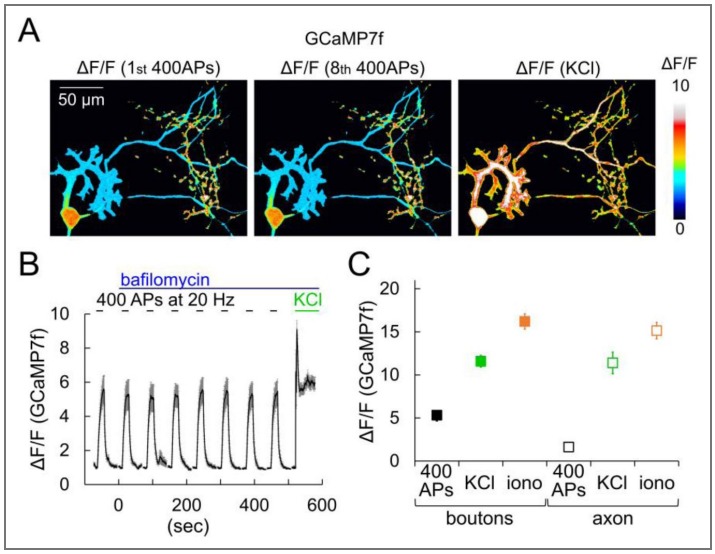


**Figure 8—figure supplement 1.** **$Ca^{2+}$ influx induced by AP trains, external high $K^+$ or ionomycin**

(**A**) Color-coded relative fluorescence increase of GCaMP7f (ΔF/F) upon 400 APs at 20 Hz (at the $1_{st}$ round or the $8_{th}$) or the following KCl application (finally 50 mM). (**B**) Time course of GCaMP7f ΔF/F upon the repetitive 400 APs trains and KCl before and after application of bafilomycin. (**C**) GCaMP7f ΔF/F at boutons on axons upon 400 APs, application of KCl or of ionomycin (iono). n = 35 (400APs), 10 (KCl) and 20 (ionomycin) boutons, or 41 (400 APs), 15 (KCl) and 26 (ionomycin) sites in axon. Data are mean ± SEM.

# Data availability

The source data supporting the findings of this study are available at KURENAI (*https://repository.kulib.kyoto-u.ac.jp/home*) via the following private link, which provides access for reviewers and editors during peer review (will be fully open at the publication). *https://openaccess.kulib.kyoto-u.ac.jp/private/e47bef052904c1f8ebd8cec9055d39598e27294e*

# Acknowledgements

We thank Drs. Mitsuharu Midorikawa and Federico Trigo for the critical reading of the manuscript and helpful comments.

# Additional information

## Funding

Japan Society for the Promotion of Science, KAKENHI grants 25K02362 (SK), 25H02611 (SK), 22H02721 (SK), 22K19360 (SK), 24K18217 (TI) and 21K15189 (TI). Takeda Science Foundation (SK). Naito Foundation (SK).

## Funding



| Funder | Grant reference number | Author |
|---|---|---|
| Japan Society for the Promotion of Science | 25K02362 | Shin-ya Kawaguchi |
| MEXT \| Japan Society for the Promotion of Science (JSPS) | 25H02611 | Shin-ya Kawaguchi |
| MEXT \| Japan Society for the Promotion of Science (JSPS) | 22H02721 | Shin-ya Kawaguchi |
| MEXT \| Japan Society for the Promotion of Science (JSPS) | 22K19360 | Shin-ya Kawaguchi |
| MEXT \| Japan Society for the Promotion of Science (JSPS) | 24K18217 | Takuma Inoshita |
| MEXT \| Japan Society for the Promotion of Science (JSPS) | 21K15189 | Takuma Inoshita |
| Takeda Science Foundation (TSF) | | Shin-ya Kawaguchi |
| Naito Foundation (内藤記念科学振興財団) | | Shin-ya Kawaguchi |



## Author ORCID iDs

**Shin-ya Kawaguchi**: https://orcid.org/0000-0002-8386-1185

# References

**Abbott LF,** Regehr WG (2004) Synaptic computation. *Nature* **431**:796-803 https://doi.org/10.1038/nature03010 | PubMed

**Adler EM,** Augustine GJ, Duffy SN, Charlton MP (1991) Alien intracellular calcium chelators attenuate neurotransmitter release at the squid giant synapse. *The Journal of Neuroscience* **11**:1496-1507 https://doi.org/10.1523/JNEUROSCI.11-06-01496.1991 | PubMed

**Ashton JC,** Friberg D, Darlington CL, Smith PF (2006) Expression of the cannabinoid CB2 receptor in the rat cerebellum: an immunohistochemical study. *Neuroscience Letters* **396**:113-116 https://doi.org/10.1016/j.neulet.2005.11.038 | PubMed

**Atwood BK,** Straiker A, MacKie K (2012) $CB_2$ cannabinoid receptors inhibit synaptic transmission when expressed in cultured autaptic neurons. *Neuropharmacology* **63**:514-523 https://doi.org/10.1016/j.neuropharm.2012.04.024 | PubMed

**Baker D,** Pryce G, Davies WL, Hiley CR (2006) In silico patent searching reveals a new cannabinoid receptor. *Trends in Pharmacological Sciences* **27**:1-4 https://doi.org/10.1016/j.tips.2005.11.003 | PubMed

**Bornschein G,** Arendt O, Hallermann S, Brachtendorf S, Eilers J, Schmidt H (2013) Paired-pulse facilitation at recurrent Purkinje neuron synapses is independent of calbindin and parvalbumin during high-frequency activation. *The Journal of Physiology* **591**:3355-3370 https://doi.org/10.1113/jphysiol.2013.254128 | PubMed

**Borst JG,** Sakmann B (1996) Calcium influx and transmitter release in a fast CNS synapse. *Nature* **383**:431-434 https://doi.org/10.1038/383431a0 | PubMed

**Bowery NG,** Bettler B, Froestl W, Gallagher JP, Marshall F, Raiteri M, Bonner TI, Enna SJ (2002) International Union of Pharmacology. XXXIII. Mammalian gamma-aminobutyric acid(B) receptors: structure and function. *Pharmacological Reviews* **54**:247-264 https://doi.org/10.1124/pr.54.2.247 | PubMed

**Brenneman DE,** Petkanas D, Ippolito M, Ward SJ (2025) Effect of Fatty Acyl Composition for Lysophosphatidylinositol on Neuroinflammatory Responses in Primary Neuronal Cultures. *Journal of Molecular Neuroscience* **75**:35 https://doi.org/10.1007/s12031-025-02326-7 | PubMed

**Castillo PE,** Younts TJ, Chávez AE, Hashimotodani Y (2012) Endocannabinoid signaling and synaptic function. *Neuron* **76**:70-81 https://doi.org/10.1016/j.neuron.2012.09.020 | PubMed

**Cazares VA,** Njus MM, Manly A, Saldate JJ, Subramani A, Ben-Simon Y, Sutton MA, Ashery U, Stuenkel EL (2016) Dynamic Partitioning of Synaptic Vesicle Pools by the SNARE-Binding Protein Tomosyn. *The Journal of Neuroscience* **36**:11208-11222 https://doi.org/10.1523/JNEUROSCI.1297-16.2016 | PubMed

**Daly CJ,** Ross RA, Whyte J, Henstridge CM, Irving AJ, McGrath JC (2010) Fluorescent ligand binding reveals heterogeneous distribution of adrenoceptors and 'cannabinoid-like' receptors in small arteries. *British Journal of Pharmacology* **159**:787-796 https://doi.org/10.1111/j.1476-5381.2009.00608.x | PubMed

**Denis Völker JS,** Micluția IV, Vinași RC (2024) Investigating Cannabidiol's potential as a supplementary treatment for schizophrenia: A narrative review. *European Journal of Pharmacology* **979**:176821 https://doi.org/10.1016/j.ejphar.2024.176821 | PubMed

**Devinsky O,** Jones NA, Cunningham MO, Jayasekera BAP, Devore S, Whalley BJ (2024) Cannabinoid treatments in epilepsy and seizure disorders. *Physiological Reviews* **104**:591-649 https://doi.org/10.1152/physrev.00049.2021 | PubMed

**Di Marzo V,** Goparaju SK, Wang L, Liu J, Bátkai S, Járai Z, Fezza F, Miura GI, Palmiter RD, Sugiura T, *et al.* (2001) Leptin-regulated endocannabinoids are involved in maintaining food intake. *Nature* **410**:822-825 https://doi.org/10.1038/35071088 | PubMed

**Diana MA,** Levenes C, Mackie K, Marty A (2002) Short-term retrograde inhibition of GABAergic synaptic currents in rat Purkinje cells is mediated by endogenous cannabinoids. *The Journal of Neuroscience* **22**:200-208 https://doi.org/10.1523/JNEUROSCI.22-01-00200.2002 | PubMed

**Díaz-Rojas F,** Sakaba T, Kawaguchi SY (2015) $Ca^{2+}$ current facilitation determines short-term facilitation at inhibitory synapses between cerebellar Purkinje cells. *The Journal of Physiology* **593**:4889-4904 https://doi.org/10.1113/JP270704 | PubMed

**Fernandez-Alfonso T,** Ryan TA (2008) A heterogeneous "resting" pool of synaptic vesicles that is dynamically interchanged across boutons in mammalian CNS synapses. *Brain Cell Biology* **36**:87-100 https://doi.org/10.1007/s11068-008-9030-y | PubMed

**Fierro L,** Llano I (1996) High endogenous calcium buffering in Purkinje cells from rat cerebellar slices. *The Journal of Physiology* **496**:617-625 https://doi.org/10.1113/jphysiol.1996.sp021713 | PubMed

**Fukaya R,** Maglione M, Sigrist SJ, Sakaba T (2021) Rapid $Ca^{2+}$ channel accumulation contributes to cAMP-mediated increase in transmission at hippocampal mossy fiber synapses. *PNAS* **118**:e2016754118 https://doi.org/10.1073/pnas.2016754118 | PubMed

**Furukawa K,** Inoshita T, Kawaguchi SY (2024) Graded control of Purkinje cell outputs by cAMP through opposing actions on axonal action potential and transmitter release. *The Journal of Physiology* https://doi.org/10.1113/JP286668 | PubMed

**Gómez-Gonzalo M,** Navarrete M, Perea G, Covelo A, Martín-Fernández M, Shigemoto R, Luján R, Araque A (2015) Endocannabinoids Induce Lateral Long-Term Potentiation of Transmitter Release by Stimulation of Gliotransmission. *Cerebral Cortex* **25**:3699-3712 https://doi.org/10.1093/cercor/bhu231 | PubMed

**Gomez LC,** Kawaguchi SY, Collin T, Jalil A, Gomez MDP, Nasi E, Marty A, Llano I (2020) Influence of spatially segregated IP3-producing pathways on spike generation and transmitter release in Purkinje cell axons. *PNAS* **117**:11097-11108 https://doi.org/10.1073/pnas.2000148117 | PubMed

**Guo J,** Ikeda SR (2004) Endocannabinoids modulate N-type calcium channels and G-protein-coupled inwardly rectifying potassium channels via CB1 cannabinoid receptors heterologously expressed in mammalian neurons. *Molecular Pharmacology* **65**:665-674 https://doi.org/10.1124/mol.65.3.665 | PubMed

**Harada K,** Kitaguchi T, Kamiya T, Aung KH, Nakamura K, Ohta K, Tsuboi T (2017) Lysophosphatidylinositol-induced activation of the cation channel TRPV2 triggers glucagon-like peptide-1 secretion in enteroendocrine L cells. *The Journal of Biochemistry* **292**:10855-10864 https://doi.org/10.1074/jbc.M117.788653 | PubMed

**Henstridge CM,** Balenga NA, Ford LA, Ross RA, Waldhoer M, Irving AJ (2008) The GPR55 ligand L-alpha-lysophosphatidylinositol promotes RhoA-dependent $Ca^{2+}$ signaling and NFAT activation. *The FASEB Journal* **23**:183-193 https://doi.org/10.1096/fj.08-108670 | PubMed

**Higashi R,** Morita M, Kawaguchi SY (2024) $Cl^-$-dependent amplification of excitatory synaptic potentials at distal dendrites revealed by voltage imaging. *Science Advances* **10**:eadj2547 https://doi.org/10.1126/sciadv.adj2547 | PubMed

**Hill MN,** Patel S (2013) Translational evidence for the involvement of the endocannabinoid system in stress-related psychiatric illnesses. *Biology of Mood & Anxiety Disorders* **3**:19 https://doi.org/10.1186/2045-5380-3-19 | PubMed

**Hirono M,** Yanagawa Y (2021) Endocannabinoids regulate cerebellar GABAergic transmission in a synapse type-dependent manner. *Journal of Neuroscience Research* **99**:898-913 https://doi.org/10.1002/jnr.24765 | PubMed

**Hosoi N,** Sakaba T, Neher E (2007) Quantitative analysis of calcium-dependent vesicle recruitment and its functional role at the calyx of Held synapse. *The Journal of Neuroscience* **27**:14286-14298 https://doi.org/10.1523/JNEUROSCI.4122-07.2007 | PubMed

**Joberty G,** Fälth-Savitski M, Paulmann M, Bösche M, Doce C, Cheng AT, Drewes G, Grandi P (2020) A Tandem Guide RNA-Based Strategy for Efficient CRISPR Gene Editing of Cell Populations with Low Heterogeneity of Edited Alleles. *The CRISPR Journal* **3**:123-134 https://doi.org/10.1089/crispr.2019.0064 | PubMed

**Kandel ER** (2001) The molecular biology of memory storage: a dialogue between genes and synapses. *Science* **294**:1030-1038 https://doi.org/10.1126/science.1067020 | PubMed

**Kano M,** Ohno-Shosaku T, Hashimotodani Y, Uchigashima M, Watanabe M (2009) Endocannabinoid-mediated control of synaptic transmission. *Physiological Reviews* **89**:309-380 https://doi.org/10.1152/physrev.00019.2008 | PubMed

**Kargl J,** Brown AJ, Andersen L, Dorn G, Schicho R, Waldhoer M, Heinemann A (2013) A selective antagonist reveals a potential role of G protein-coupled receptor 55 in platelet and endothelial cell function. *Journal of Pharmacology and Experimental Therapeutics* **346**:54-66 https://doi.org/10.1124/jpet.113.204180 | PubMed

**Katona I,** Rancz EA, Acsady L, Ledent C, Mackie K, Hajos N, Freund TF (2001) Distribution of CB1 cannabinoid receptors in the amygdala and their role in the control of GABAergic transmission. *The Journal of Neuroscience* **21**:9506-9518 https://doi.org/10.1523/JNEUROSCI.21-23-09506.2001 | PubMed

**Kawaguchi SY,** Hirano T (2007) Sustained structural change of GABA(A) receptor-associated protein underlies long-term potentiation at inhibitory synapses on a cerebellar Purkinje neuron. *Journal of Neuroscience Research* **27**:6788-99 https://doi.org/10.1523/JNEUROSCI.1981-07.2007 | PubMed

**Kawaguchi SY,** Sakaba T (2015) Control of inhibitory synaptic outputs by low excitability of axon terminals revealed by direct recording. *Neuron* **85**:1273-1288 https://doi.org/10.1016/j.neuron.2015.02.013 | PubMed

**Kew JN,** Ducarre JM, Pflimlin MC, Mutel V, Kemp JA (2001) Activity-dependent presynaptic autoinhibition by group II metabotropic glutamate receptors at the perforant path inputs to the dentate gyrus and CA1. *Neuropharmacology* **40**:20-27 https://doi.org/10.1016/s0028-3908(00)00118-0 | PubMed

**Khan AA,** Shekh-Ahmad T, Khalil A, Walker MC, Ali AB (2018) Cannabidiol exerts antiepileptic effects by restoring hippocampal interneuron functions in a temporal lobe epilepsy model. *British Journal of Pharmacology* **175**:2097-2115 https://doi.org/10.1111/bph.14202 | PubMed

**Kim SH,** Ryan TA (2010) CDK5 serves as a major control point in neurotransmitter release. *Neuron* **67**:797-809 https://doi.org/10.1016/j.neuron.2010.08.003 | PubMed

**Kreitzer AC,** Regehr WG (2001) Retrograde inhibition of presynaptic calcium influx by endogenous cannabinoids at excitatory synapses onto Purkinje cells. *Neuron* **29**:717-727 https://doi.org/10.1016/s0896-6273(01)00246-x | PubMed

**Kushmerick C,** Price GD, Taschenberger H, Puente N, Renden R, Wadiche JI, Duvoisin RM, Grandes P, von Gersdorff H (2004) Retroinhibition of Presynaptic $Ca^{2+}$ Currents by Endocannabinoids Released via Postsynaptic mGluR Activation at a Calyx Synapse. *The Journal of Neuroscience* **24**:5955 https://doi.org/10.1523/JNEUROSCI.0768-04.2004 | PubMed

**Lee JS,** Ho WK, Lee SH (2012) Actin-dependent rapid recruitment of reluctant synaptic vesicles into a fast-releasing vesicle pool. *PNAS* **109**:765-774 https://doi.org/10.1073/pnas.1114072109 | PubMed

**Mori Y,** Takenaka KI, Fukazawa Y, Takamori S (2021) The endosomal Q-SNARE, *Syntaxin* 7, defines a rapidly replenishing synaptic vesicle recycling pool in hippocampal neurons. *Communications Biology* **4**:981 https://doi.org/10.1038/s42003-021-02512-4 | PubMed

**Midorikawa M,** Sakamoto H, Nakamura Y, Hirose K, Miyata M (2024) Developmental refinement of the active zone nanotopography and axon wiring at the somatosensory thalamus. *Cell Reports* **43**:114770 https://doi.org/10.1016/j.celrep.2024.114770 | PubMed

**Miki T,** Malagon G, Pulido C, Llano I, Neher E, Marty A (2016) Actin- and Myosin-Dependent Vesicle Loading of Presynaptic Docking Sites Prior to Exocytosis. *Neuron* **91**:808-823 https://doi.org/10.1016/j.neuron.2016.07.033 | PubMed

**Neher E,** Marty A (1982) Discrete changes of cell membrane capacitance observed under conditions of enhanced secretion in bovine adrenal chromaffin cells. *PNAS* **79**:6712-6716 https://doi.org/10.1073/pnas.79.21.6712 | PubMed

**Neher E,** Sakaba T (2001) Combining deconvolution and noise analysis for the estimation of transmitter release rates at the calyx of held. *Journal of Neuroscience* **21**:444-461 https://doi.org/10.1523/JNEUROSCI.21-02-00444.2001 | PubMed

**Nicholson-Tomishima K,** Ryan TA (2004) Kinetic efficiency of endocytosis at mammalian CNS synapses requires synaptotagmin I. *PNAS* **101**:16648-16652 https://doi.org/10.1073/pnas.0406968101 | PubMed

**Ohno-Shosaku T,** Maejima T, Kano M (2001) Endogenous cannabinoids mediate retrograde signals from depolarized postsynaptic neurons to presynaptic terminals. *Neuron* **29**:729-738 https://doi.org/10.1016/s0896-6273(01)00247-1 | PubMed

**Oka S,** Nakajima K, Yamashita A, Kishimoto S, Sugiura T (2007) Identification of GPR55 as a lysophosphatidylinositol receptor. *Biochemical and Biophysical Research Communications* **362**:928-934 https://doi.org/10.1016/j.bbrc.2007.08.078 | PubMed

**Oka S,** Toshida T, Maruyama K, Nakajima K, Yamashita A, Sugiura T (2009) 2-Arachidonoyl-sn-glycero-3-phosphoinositol: a possible natural ligand for GPR55. *The Journal of Biochemistry* **145**:13-20 https://doi.org/10.1093/jb/mvn136 | PubMed

**Ramírez-Franco J,** Bartolomé-Martín D, Alonso B, Torres M, Sánchez-Prieto J (2014) Cannabinoid type 1 receptors transiently silence glutamatergic nerve terminals of cultured cerebellar granule cells. *PLoS One* **9**:e88594 https://doi.org/10.1371/journal.pone.0088594 | PubMed

**Ran FA,** Hsu PD, Wright J, Agarwala V, Scott DA, Zhang F (2013) Genome engineering using the CRISPR-Cas9 system. *Natureprotocols* **8**:2281-2308 https://doi.org/10.1038/nprot.2013.143 | PubMed

**Rosenberg EC,** Chamberland S, Bazelot M, Nebet ER, Wang X, McKenzie S, Jain S, Greenhill S, Wilson M, Marley N, *et al.* (2023) Cannabidiol modulates excitatory-inhibitory ratio to counter hippocampal hyperactivity. *Neuron* **111**:1282-1300.e8. https://doi.org/10.1016/j.neuron.2023.01.018 | PubMed

**Ryberg E,** Larsson N, Sjögren S, Hjorth S, Hermansson NO, Leonova J, Elebring T, Nilsson K, Drmota T, Greasley PJ (2007) The orphan receptor GPR55 is a novel cannabinoid receptor. *British Journal of Pharmacology* **152**:1092-1101 https://doi.org/10.1038/sj.bjp.0707460 | PubMed

**Sakaba T** (2006) Roles of the fast-releasing and the slowly releasing vesicles in synaptic transmission at the calyx of Held. *The Journal of Neuroscience* **26**:5863-5871 https://doi.org/10.1523/JNEUROSCI.0182-06.2006 | PubMed

**Sankaranarayanan S,** Ryan TA (2000) Real-time measurements of vesicle-SNARE recycling in synapses of the central nervous system. *Nature Cell Biology* **2**:197-204 https://doi.org/10.1038/35008615 | PubMed

**Sankaranarayanan S,** Ryan TA (2001) Calcium accelerates endocytosis of vSNAREs at hippocampal synapses. *Nature Neuroscience* **4**:129-36 https://doi.org/10.1038/83949 | PubMed

**Schneggenburger R,** Neher E (2000) Intracellular calcium dependence of transmitter release rates at a fast central synapse. *Nature* **406**:889-893 https://doi.org/10.1038/35022702 | PubMed

**Shallcross J,** Hámor P, Bechard AR, Romano M, Knackstedt L, Schwendt M (2019) The Divergent Effects of CDPPB and Cannabidiol on Fear Extinction and Anxiety in a Predator Scent Stress Model of PTSD in Rats. *Frontiers in Behavioral Neuroscience* **13**:91 https://doi.org/10.3389/fnbeh.2019.00091 | PubMed

**Shirai Y,** Ito M (2004) Specific differential expression of phospholipase A2 subtypes in rat cerebellum. *Journal of Neurocytology* **33**:297-307 https://doi.org/10.1023/B:NEUR.0000044191.83858.f7 | PubMed

**Sylantyev S,** Jensen TP, Ross RA, Rusakov DA (2013) Cannabinoid- and lysophosphatidylinositol-sensitive receptor GPR55 boosts neurotransmitter release at central synapses. *PNAS* **110**:5193-5198 https://doi.org/10.1073/pnas.1211204110 | PubMed

**Takahashi T,** Kajikawa Y, Tsujimoto T (1998) G-Protein-coupled modulation of presynaptic calcium currents and transmitter release by a GABAB receptor. *The Journal of Neuroscience* **18**:3138-3146 https://doi.org/10.1523/JNEUROSCI.18-09-03138.1998 | PubMed

**Tran V,** Silva M, Marty A (2023) Prioritized docking of synaptic vesicles provided by a rapid recycling pathway. *iScience* **26**:106366 https://doi.org/10.1016/j.isci.2023.106366 | PubMed

**Tsou K,** Brown S, Sañudo-Peña MC, Mackie K, Walker JM (1998) Immunohistochemical distribution of cannabinoid CB1 receptors in the rat central nervous system. *Neuroscience* **83**:393-411 https://doi.org/10.1016/s0306-4522(97)00436-3 | PubMed

**Uusisaari M,** Obata K, Knöpfel T (2006) Morphological and electrophysiological properties of GABAergic and non-GABAergic cells in the deep cerebellar nuclei. *Journal of Neurophysiology* **97**:901-911 https://doi.org/10.1152/jn.00974.2006 | PubMed

**Vyleta NP,** Jonas P (2014) Loose coupling between $Ca^{2+}$ channels and release sensors at a plastic hippocampal synapse. *Science* **343**:665-670 https://doi.org/10.1126/science.1244811 | PubMed

**Weisskopf MG,** Castillo PE, Zalutsky RA, Nicoll RA (1994) Mediation of hippocampal mossy fiber long-term potentiation by cyclic AMP. *Science* **265**:1878-1882 https://doi.org/10.1126/science.7916482 | PubMed

**Wilson RI,** Nicoll RA (2001) Endogenous cannabinoids mediate retrograde signalling at hippocampal synapses. *Nature* **410**:588-592 https://doi.org/10.1038/35069076 | PubMed

**Wu CS,** Chen H, Sun H, Zhu J, Jew CP, Wager-Miller J, Straiker A, Spencer C, Bradshaw H, Mackie K, *et al.* (2013) GPR55, a G-protein coupled receptor for lysophosphatidylinositol, plays a role in motor coordination. *PLoS One* **8**:e60314 https://doi.org/10.1371/journal.pone.0060314 | PubMed

**Wu Y,** Liu Q, Guo B, Ye F, Ge J, Xue L (2020) BDNF Activates Postsynaptic TrkB Receptors to Induce Endocannabinoid Release and Inhibit Presynaptic Calcium Influx at a Calyx-Type Synapse. *The Journal of Neuroscience* **40**:8070-8087 https://doi.org/10.1523/JNEUROSCI.2838-19.2020 | PubMed

**Xia R,** Yuan Q, Wang N, Hou L, Abe J, Song J, Ito Y, Xu HE, He Y (2025) Structural insight into GPR55 ligand recognition and G-protein coupling. *Cell Research* **35**:76-79 https://doi.org/10.1038/s41422-024-01044-w | PubMed

**Yamashita M,** Kawaguchi SY, Hori T, Takahashi T (2018) Vesicular GABA Uptake Can Be Rate Limiting for Recovery of IPSCs from Synaptic Depression. *Cell Reports* **22**:3134-3141 https://doi.org/10.1016/j.celrep.2018.02.080 | PubMed

**Yamashita A,** Kumazawa T, Koga H, Suzuki N, Oka S, Sugiura T (2010) Generation of lysophosphatidylinositol by DDHD domain containing 1 (DDHD1): Possible involvement of phospholipase D/phosphatidic acid in the activation of DDHD1. *Molecular and Cell Biology of Lipids* **1801**:711-720 https://doi.org/10.1016/j.bbalip.2010.03.012 | PubMed

**Zorrilla de San Martin J,** Trigo FF, Kawaguchi SY (2017) Axonal GABAA receptors depolarize presynaptic terminals and facilitate transmitter release in cerebellar Purkinje cells. *The Journal of Physiology* **595**:7477-7493 https://doi.org/10.1113/JP275369 | PubMed

# Peer reviews

## Reviewer #1 (Public review):

In this manuscript, the authors report that GPR55 activation in presynaptic terminals of Purkinje cells decrease GABA release at the PC-DCN synapse. The authors use an impressive array of techniques (including highly challenging presynaptic recordings) to show that GPR55 activation reduces the readily releasable pool of vesicle without affecting presynaptic AP waveform and presynaptic Ca2+ influx. This is an interesting study, which is seemingly well-executed and proposes a novel mechanism for the control of neurotransmitter release. However, the authors' main conclusions are heavily, if not solely, based on pharmacological agents that most often than not demonstrate affinity at multiple targets. Below are points that the authors should consider in a revised version.

Major points:

(1) There is no clear evidence that GPR55 is specifically expressed in presynaptic terminals at the PC-DCN synapse. The authors cited Ryberg 2007 and Wu 2013 in the introduction, mentioning that GPR55 is potentially expressed in PCs. Ryberg (2007) offers no such evidence, and the expression in PC suggested by Wu (2013) does not necessarily correlate with presynaptic expression. The authors should perform additional experiments to demonstrate presynaptic expression of GPR55 at PC-DCN synapse.

(2) The authors' conclusions rest heavily on pharmacological experiments, with compounds that are sometimes not selective for single targets. Genetic deletion of GPR55 would be a more appropriate control. The authors should also expand their experiments with occlusion experiments, showing if the effects of LPI are absent after AM251 or O-1602 treatment. In

addition, the authors may want to consider AM281 as a CB1R antagonist without reported effects at GPR55.

(3) It is not clear how long the different drugs were applied, and at what time the recording were performed during or following drug application. It appears that GPR55 agonists can have transient effects (Sylantyev, 2013; Rosenberg, 2023), possibly due to receptor internalization. The timeline of drug application should be reported, where IPSC amplitude is shown as a function of time and drug application windows are illustrated.

(4) A previous investigation on the role of GPR55 in the control of neurotransmitter release is not cited nor discussed Sylantyev et al., (2013, PNAS, Cannabinoid- and lysophosphatidylinositol-sensitive receptor GPR55 boosts neurotransmitter release at central synapses). Similarities and differences should be discussed.

Minor point:

(1) What is the source of LPI? What isoform was used? The multiple isoforms of LPI have different affinities for GPR55.

Comments on revisions:

In this revised version, the authors have addressed my major concerns. Notably, they used CRISPR/Cas9 genetic knockdown of GPR55 to independently validate their original findings. The main conclusions are now well supported and represent an important contribution to the field.

https://doi.org/10.7554/eLife.105268.2.sa3

## Reviewer #2 (Public review):

Summary:

This paper investigates the mode of action of GPR55, a relatively understudied type of cannabinoid receptors, in presynaptic terminals of Purkinje cells. The authors use demanding techniques of patch clamp recording of the terminals, sometimes coupled with another recording of the postsynaptic cell. They find a lower release probability of synaptic vesicles after activation of GPR55 receptors, while presynaptic voltage-dependent calcium currents are unaffected. They propose that the size of a specific pool of synaptic vesicles supplying release sites is decreased upon activation of GPR55 receptors.

Strengths:

The paper uses cutting edge techniques to shed light on a little studied, potentially important type of cannabinoid receptors. The results are clearly presented, and the conclusions are sound.

Weaknesses:

The nature of the vesicular pool that is modified following activation of GPR55 is not definitively characterized.

Comments on revisions:

The authors have done a good job in answering the criticisms of reviewers. Consequently, the revised version offers a substantial improvement over the first version.

https://doi.org/10.7554/eLife.105268.2.sa2

## Reviewer #3 (Public review):

Inoshita and Kawaguchi investigated the effects of GPR55 activation on synaptic transmission in vitro. To address this question, they performed direct patch-clamp recordings from axon terminals of cerebellar Purkinje cells and fluorescent imaging of vesicular exocytosis utilizing synapto-pHluorin. They found that exogenous activation of GPR55 suppresses GABA release at Purkinje cell to deep cerebellar nuclei (PC-DCN) synapses by reducing the readily releasable pool (RRP) of vesicles. This mechanism may also operate at other synapses.

Strengths:

The main strength of this study lies in combining patch-clamp recordings from axon terminals with imaging of presynaptic vesicular exocytosis to reveal a novel mechanism by which activation of GPR55 suppresses inhibitory synaptic strength. The results strongly suggest that GPR55 activation reduces the RRP size without altering presynaptic calcium influx.

Weaknesses:

The study relies on the exogenous application of GPR55 agonists. It remains unclear whether endogenous ligands released by physiological or pathological processes would have similar effects. There is also little evidence that GPR55 is expressed in Purkinje cell axon boutons. This study would benefit from the use of GPR55 knockout (KO) mice. The downstream mechanism by which GPR55 mediates the suppression of GABA release remains unknown.

Comments on revisions:

The authors have addressed all my concerns effectively. I have no further comments and want to commend their comprehensive study.

https://doi.org/10.7554/eLife.105268.2.sa1

## Author response:

The following is the authors' response to the original reviews

> ***Public Reviews:***
>
> ***Reviewer #1 (Public review):***
>
> *In this manuscript, the authors report that GPR55 activation in presynaptic terminals of Purkinje cells decrease GABA release at the PC-DCN synapse. The authors use an impressive array of techniques (including highly challenging presynaptic recordings) to show that GPR55 activation reduces the readily releasable pool of vesicle without affecting presynaptic AP waveform and presynaptic $Ca^{2+}$ influx. This is an interesting study, which is seemingly well-executed and proposes a novel mechanism for the control of neurotransmitter release. However, the authors' main conclusions are heavily, if not solely, based on pharmacological agents that most often than not demonstrate affinity at multiple targets. Below are points that the authors should consider in a revised version.*

We are happy to hear the encouraging comments from this reviewer, and thank for pointing out the important issues including the previous study design depending only on pharmacological agents. To address these, we have performed additional experiments, as detailed below.

> *Major points:*

> *(1) There is no clear evidence that GPR55 is specifically expressed in presynaptic terminals at the PC-DCN synapse. The authors cited Ryberg 2007 and Wu 2013 in the introduction, mentioning that GPR55 is potentially expressed in PCs. Ryberg (2007) offers no such evidence, and the expression in PC suggested by Wu (2013) does not necessarily correlate with presynaptic expression. The authors should perform additional experiments to demonstrate the presynaptic expression of GPR55 at PC-DCN synapse.*

We completely agree with the reviewer in that our previous manuscript lacked the reliable information regarding presynaptic expression of GPR55 at PC boutons.

To clarify the localization, we first tried immunostaining of GPR55 using commercially available antibodies, but unfortunately they did not provide clear labeling of neurons and also even in GPR55-transfected HEK cells (used as positive control). Thus, we gave up the direct immunostaining. Alternatively, we attempted to label PC axonal boutons by GPR55-targeting dye together with a complementary strategy based on gene knock-down. Specifically, we used T1117, a fluorescent derivative of AM251 which is a GPR55 ligand used in the manuscript, and clear fluorescent signals were evident at GFP-labeled PC terminals. Still, by itself it was not clear whether the labeling was mediated by association with GPR55. Therefore, we also attempted to specifically suppress gene expression of GPR55 using CRISPR/Cas9-mediated genome editing in PCs, based on acute DNA micro-injection of plasmids into nuclei of PCs to express gRNAs targeting GPR55 together with Cas9. As a result, 5 days after the knock-down, T1117 labeling at axon terminals was reduced by ~50% compared to Cas9-alone controls. All these data are now shown in new Figure 2, and explained in the text p5-6, lines 141-159. Further, the reduction of GPR55 expression abolished the AM251-mediated reduction of vesicular exocytosis, as shown in new Figure 3D, E.

Taken together, these results essentially convince our main conclusions by strongly suggesting that GPR55 is present at PC axon terminals, where it negatively regulates the exocytosis upon activation by AM251.

> *(2) The authors' conclusions rest heavily on pharmacological experiments, with compounds that are sometimes not selective for single targets. Genetic deletion of GPR55 would be a more appropriate control. The authors should also expand their experiments with occlusion experiments, showing if the effects of LPI are absent after AM251 or O-1602 treatment. In addition, the authors may want to consider AM281 as a CB1R antagonist without reported effects at GPR55.*

We thank the reviewer for pointing out these important issues. First, as noted above to confirm the presence of GPR55 at axon terminals of PCs, we performed genetic deletion of GPR55 using CRISPR/Cas9 system. In PCs co-expressing Cas9 and two gRNAs targeting the ligand-binding domain of GPR55, AM251 failed to suppress the exocytosis at PC boutons, together with decreased T1117 labeling. Therefore, the idea that GPR55 negatively regulates transmitter release at PC boutons has now been strengthened. The new data is shown in Figure 3D and E, and explained in the text p6, lines 173-178.

As suggested, we also carried out the occlusion experiments with LPI and AM251. First, LPI similarly reduced the readily releasable pool (RRP) size as AM251 did. Then, applied together, LPI and AM251 did not further reduce the RRP size compared with the effect by either compound alone. Thus, LPI and AM251 seem to act through the same pathway, consistent with the idea for role of GPR55 activation. The data is shown in new Figure 5—figure supplement 1 and explained in the text, p7-8, lines 215-221.

Regarding another point suggested by the reviewer, we applied AM281 and observed no effect on transmission at the PC–target neuron synapses (shown in new Figure 1F and I;

explained in the text p5, lines 117-123), indicating that the effect of AM251 is likely to be mediated by GPR55, but not by CB1R.

Taken together, our additional experiments based on genetic and pharmacological experiments have consolidated our conclusion that GPR55 suppresses the presynaptic neurotransmitter release in PC boutons.

> *(3) It is not clear how long the different drugs were applied, and at what time the recordings were performed during or following drug application. It appears that GPR55 agonists can have transient effects (Sylantyev, 2013; Rosenberg, 2023), possibly due to receptor internalization. The timeline of drug application should be reported, where IPSC amplitude is shown as a function of time and drug application windows are illustrated.*

Thank you for suggesting the better presentation of data. Accordingly, we have re-organized figures showing time course of changes in IPSCs before and after the drug application (new Figure 1 and 4; p4, lines 94-97; p5, lines 110-115; p7, lines 193-197). The current data presentation clearly shows that the effect of AM251 becomes evident in a few minutes after application, and somehow reaches a saturated level.

> *(4) A previous investigation on the role of GPR55 in the control of neurotransmitter release is not cited nor discussed (Sylantyev et al., (2013, PNAS, Cannabinoid- and lysophosphatidylinositolsensitive receptor GPR55 boosts neurotransmitter release at central synapses). Similarities and differences should be discussed.*

We are really sorry for failing to adequately discuss this important work in our previous manuscript, and deeply appreciate the reviewer for pointing this out. We have now cited and discussed the work by Sylantyev et al. (2013), in the text (p12, lines 380-389), as following:

'Pioneering studies clarified an important role of GPR55 in synaptic transmission at hippocampal excitatory synapses, demonstrating presynaptic enhancement of glutamate release presumably by elevating the cytoplasmic residual $Ca^{2+}$ via release from intracellular stores (Sylantyev et al., 2013; Rosenberg et al., 2023), in contrast to the suppression of release in our observation. The lack of positive modulation of AP-triggered release through residual $Ca^{2+}$ in PC terminals might be due to abundant amount of potent $Ca^{2+}$ buffer calbindin (Fierro and Llano, 1996). Indeed, increased vesicular fusion only for the AP-insensitive spontaneous vesicular release (as mIPSCs) was observed upon the $IP_3$-mediated $Ca^{2+}$ release from internal store (Gomez et al., 2020). Thus, minimal sensitivity of AP-triggered release to residual $Ca^{2+}$ in PC boutons would underlie the distinct effects of GPR55 activation at the presynaptic side.'

> *Minor point:*
>
> *(1) What is the source of LPI? What isoform was used? The multiple isoforms of LPI have different affinities for GPR55.*

Thank you for letting us know about the lack of important information in the previous manuscript. In our experiments, we used a soybean-derived LPI mixture containing approximately 58% C16:0 and 42% C18:0 or C18:2 species. According to Brenneman et al. (2025), these isoforms show moderate or strong effects in cultured DRG neurons, whereas the C20:4 isoform, reported to promote neuroinflammatory signaling, was contained only at very low levels. We have added this information to the revised manuscript and briefly discussed the influence of different LPI isoforms on the physiological outcomes of GPR55 activation (p5, lines 127-131; p15, lines 493-496).

> ***Reviewer #2 (Public review):***
>
> *Summary:*

> *This paper investigates the mode of action of GPR55, a relatively understudied type of cannabinoid receptor, in presynaptic terminals of Purkinje cells. The authors use demanding techniques of patch clamp recording of the terminals, sometimes coupled with another recording of the postsynaptic cell. They find a lower release probability of synaptic vesicles after activation of GPR55 receptors, while presynaptic voltage-dependent calcium currents are unaffected. They propose that the size of a specific pool of synaptic vesicles supplying release sites is decreased upon activation of GPR55 receptors.*
>
> *Strengths:*
>
> *The paper uses cutting-edge techniques to shed light on a little-studied, potentially important type of cannabinoid receptor. The results are clearly presented, and the conclusions are for the most part sound.*

We feel very happy to see the positive comments from the reviewer.

> *Weaknesses:*
>
> *The nature of the vesicular pool that is modified following activation of GPR55 is not definitively characterized.*

We agree with the reviewer in that our data cannot fully address the changes of vesicle pools caused by GPR55. As detailed in responses to comments in 'Recommendations for the authors' from the reviewer, we have added explanation and discussion in the main text of the revised manuscript.

> ***Reviewer #3 (Public review):***
>
> *Summary:*
>
> *Inoshita and Kawaguchi investigated the effects of GPR55 activation on synaptic transmission in vitro. To address this question, they performed direct patch-clamp recordings from axon terminals of cerebellar Purkinje cells and fluorescent imaging of vesicular exocytosis utilizing synaptopHluorin. They found that exogenous activation of GPR55 suppresses GABA release at Purkinje cell to deep cerebellar nuclei (PC-DCN) synapses by reducing the readily releasable pool (RRP) of vesicles. This mechanism may also operate at other synapses.*
>
> *Strengths:*
>
> *The main strength of this study lies in combining patch-clamp recordings from axon terminals with imaging of presynaptic vesicular exocytosis to reveal a novel mechanism by which activation of GPR55 suppresses inhibitory synaptic strength. The results strongly suggest that GPR55 activation reduces the RRP size without altering presynaptic calcium influx.*

We thank the reviewer for giving the encouraging comments on our study.

> *Weaknesses:*

> *The study relies on the exogenous application of GPR55 agonists. It remains unclear whether endogenous ligands released due to physiological or pathological activities would have similar effects. There is no information regarding the time course of the agonist-induced suppression. There is also little evidence that GPR55 is expressed in Purkinje cells. This study would benefit from using GPR55 knockout (KO) mice. The downstream mechanism by which GPR55 mediates the suppression of GABA release remains unknown.*

We thank the reviewer for pointing out all of these important issues to be ideally addressed. As detailed in the responses to comments in the 'Recommendations for the authors' from the reviewers, we have addressed most of these weak points, and also added careful discussion in the text about the open questions to be solved in the future study.

> ***Recommendations for the authors:***
>
> ***Reviewer #2 (Recommendations for the authors):***
>
> *This is a high-quality paper that reports novel and interesting results. The authors should consider one main critique, related to Figure 6, as well as a number of minor points.*

We thank the reviewer for making very positive assessment of our study. We have carefully considered the main critique regarding presynaptic vesicle pools (related to previous Figure 6), as well as other points, and accordingly revised manuscript.

> *Main critique:*
>
> *In Figure 6, it is said that GPR55 locks SVs in a state that is insensitive to VGCCs, based on a series of experiments with synapto-pHluorin. This conclusion is open to several critiques:*
>
> *The authors' model is shown in the diagram of Figure 6A. In this scheme, it appears as if recycled SVs eventually re-acidify in spite of the presence of bafilomycin, and that they are directed to a location close to the plasma membrane, but away from VGCCs. In fact, there is no evidence that the effects of bafilomycin could be limited in time. And there is a lot of evidence indicating that recycled SVs move back to release sites, close to VGCCs.*

We are so sorry for presenting misleading figure panel in the previous Figure 6A. As the reviewer says, the effect of bafilomycin should be expected to last for long, and then the endocytosed vesicles cannot be re-acidified. Now, in new Figure 8A, we have changed the panel for explanation about the experimental situation of vesicles in the presence of bafilomycin. Another insightful point, kindly suggested by the reviewer, regarding the quick recruitment of newly endocytosed vesicles to release sites, is highly related to the interpretation of our data, but is a different issue from the situation explained in new Figure 8A. To avoid confusion, the arrow drawn in the previous version indicating the endocytosed vesicle movement back to the docked situation has been omitted in the new panel, and this critical issue is now carefully discussed in terms of the mechanism of GPR55 action on the release machinery (p15, lines 480-482).

> *The saturation of the train-induced signals is interpreted as reflecting an exhaustion of SVs initially close to VGCCs or more generally, susceptible to being released following VGCC activation.*
>
> *In an alternative scenario, saturation occurs because AP trains, or KCl applications, become unable to activate VGCCs. This could occur either because long illumination causes photodamage of VGCCs, or because repeated activation of VGCCs leads to their inactivation. The latter explanation is possible in spite of a publication from the authors'*

> *laboratory describing the facilitation of presynaptic VGCCs following paired stimulations in this synapse (Diaz-Rojas et al., 2015).*

We agree that it is an important control experiment to demonstrate that $Ca^{2+}$ increase upon repetitive AP trains is intact even during or after the long photo-illumination for imaging. To test this possibility, we have performed additional fluorescent $Ca^{2+}$ imaging at PC varicosities during individual 400-AP trains and also in response to 50 mM KCl following the series of AP trains. Now new data demonstrated that $Ca^{2+}$ influx remains constant across all AP trains (shown in Figure 8— figure supplement 1), arguing against VGCC inactivation or photodamage as a major factor underlying the saturated signal increase in the synapto-pHluorin. We have added explanation regarding this issue in the text p11, lines 327-329.

> *The authors explain the larger effect of ionomycin compared with AP trains and KCl applications as reflecting a better capacity to increase the bulk calcium concentration. The above proposal for the inactivation of VGCCs offers an alternative explanation, in my view more likely.*

As noted above, our newly added $Ca^{2+}$ imaging data clearly showed that individual AP trains induced similar $Ca^{2+}$ influxes during repetitive trials, in line with our original interpretation. In addition, the $Ca^{2+}$ increase by KCl was shown to be more potent and broader in axon terminals and trunks. Nevertheless, the exocytic signal caused by ionomycin was clearly large, implying a critical effect of the source of $Ca^{2+}$ influx in PC boutons. Therefore, we suppose that the marked effect of ionomycin on release reflects higher elevation of bulk $Ca^{2+}$ in the cytoplasm arising from non-site selective $Ca^{2+}$-ionophore (Figure 8—figure supplement 1, p11, lines 327-334; lines 342-349).

> *In yet another scenario, recycled SVs in bafilomycin retain their fluorescence since they do not reacidify, but they come back to release sites to undergo new rounds of exocytosis. The new exocytosis events do not increase the fluorescence since the pH in the vicinity of synapto-pHluorin does not change. NH4Cl would then increase the fluorescence by revealing SVs that had not undergone exocytosis-endocytosis cycles during AP trains or KCl exposure. In this last scenario, the GPR55-sensitive SV pool would be a specific sub-pool of SVs that can be recycled by repetitive 400 AP trains.*

We deeply appreciate the reviewer for pointing out this important possibility. We completely agree that this scenario can also explain the pool which is sensitive to GPR55. Therefore, we have added explanation of this possibility in the text (p15, lines 474–482).

> *Figure 6F shows calcium imaging measurements of PC varicosities. Unfortunately, crucial measurements are missing. It would have been revealing to compare calcium rises for the first and the last of the 8 400-AP trains. And to compare calcium rises elicited by 60 mM KCl before and after the series of 8 400-AP trains.*

This is an important control experiment. Therefore, we have performed additional $Ca^{2+}$ imaging during the eight 400-AP trains and KCl application. The new results shown in the present Figure 8—figure supplement 1 clearly suggest that $Ca^{2+}$ rises are comparable between the first and eighth trains, and that additional $Ca^{2+}$ influx (which was large in amplitude and wide in area) could still be evoked by KCl after the eight trains. The experiments are explained in the text p11, lines 327336.

> *Minor points:*
>
> *(1) Introduction: The Introduction would benefit from a more substantial description of what is known about GPR55 and downstream signaling pathways. Right now, it is stated that GPR55 is 'potentially expressed in PCs': What are the arguments behind this statement? Also, the signaling pathway is discussed on p.12, much too late in the ms. Why not move this section to the Introduction?*

We thank the reviewer for the helpful suggestion. As recommended, in the revised manuscript, we have changed the Introduction by moving the sentences from other sections, including speculation about the expression of GPR55 in Purkinje cells (Ryberg et al., 2007; Wu et al., 2013) (p3-4, lines 71-75) and downstream signaling pathways ($G\alpha_q$/PLC/$IP_3$/$Ca^{2+}$ and $G\alpha_{13}$/RhoA/ROCK) (p3, 63-68).

> *(2) Legend to Figures 1, 2, and 4: What is the EGTA concentration in these experiments?*

As suggested, the EGTA concentrations (0.5 or 5 mM) used in the individual experiments have now been clearly indicated both in the figure legends and in the Methods section (p18, lines 585586).

> *(3) Fig. 3C: These experiments show that some SV pool is depleted by AM251. The authors state that this is the RRP, but other options are possible. In the calyx of Held, similar experiments are supposed to deplete not only the FRP (=RRP, presumably) but also the SRP.*

We thank the reviewer for pointing out the important aspect related to category for vesicle pools. In PC boutons, the membrane capacitance increases in response to different duration of depolarization pulses in a manner fitted by a single exponential curve (see Figure 5C for example). Our previous study (Kawaguchi and Sakaba, 2015) noted that the vesicle pools corresponding to FRP and SRP may not be easy to distinguish in PCs, suggesting apparently single component. That's the reason why we simply describe the component as RRP in the present manuscript. Still, as suggested, careful discussion about typical fast- and slow components would be helpful to interpret our present findings. Therefore in the revised manuscript, we have added a sentence to explain this issue (p7, lines 211-214).

> *(4) p. 8: When the 400 APs protocol is introduced, the corresponding frequency (20 Hz?) should be mentioned. This information comes only much later in the ms.*

We are sorry for our insufficient explanation in the previous manuscript. As suggested, we have clearly written the stimulation frequency '20 Hz' in the main text where the 400 APs protocol first appears (p9, lines 277-278).

> *(5) Figure 5, panels B and F: synapto-pHluorin is labelled twice 'synapto-pHluolin'.*

Sorry for careless typos. Now, those are corrected (new Figure 7).

> *(6) Legend to Figure 5, last line: 'x' is missing in the last equation.*

Thank you for the careful and kind check. Now, 'x' has been added to the last equation in the legend for new Figure 7.

> *(7) p. 7, Interpretation of EGTA effects: The authors frame their interpretation of EGTA effects around the distance between release sites and VGCCs. However since AM251 appears to alter the recruitment of SVs, a more parsimonious interpretation would be that EGTA modifies the calciumdependent movement of SVs towards release sites.*

Thank you for suggesting an insightful scenario. We agree that the capacitance jump upon long depolarization pulse would include exocytosis of substantial amount of vesicles which

are newly recruited during the $Ca^{2+}$ increase. Then, as the reviewer states, EGTA possibly lowers the $Ca^{2+}$dependent replenishment of synaptic vesicles, and this replenishment system might be the target of GPR55 activation. Therefore, we have now clearly added an explanation about this possibility in the text (p15, lines 474-482).

> *(8) p. 13, Interpretation of GPR55 sensitive SV pool: The authors suggest a larger distance to VGCCs for this pool compared to naïve SVs. An alternative could be that in the presence of GPR55, the recruitment to release sites would be less efficient.*

This is also an insightful suggestion to speculate the causal relationship between the GPR55mediated reduction of vesicular release and the vesicle pools. Accordingly, we have revised the Discussion (see "Dynamics of synaptic vesicles among distinct functional pools") by clearly telling about the possibility of decreased recruitment of vesicles to release sites after the GPR55 activation (p15, lines 474-482). By totally considering all the suggested scenario, we believe that the possible mechanisms for GPR55-mediated reduction of release are much more clearly explained in the revised manuscript.

> ***Reviewer #3 (Recommendations for the authors):***
>
> *(1) The time course of the agonist-induced suppression should be reported (Figure 1).*

This is an important point to show data clearly, as suggested also by the reviewer 1. Accordingly, we have changed the figure panels to show time courses of agonist-induced suppression (shown in new Figures 1 and 4).

> *(2) Show that the suppression of GABAergic transmission mediated by AM251 and LPI is eliminated in GPR55 KO mice.*

We appreciate the reviewer for putting us to try this important experiment. Owing to the suggestion, we attempted to knock-down the GPR55 expression using CRISPR/Cas9 in cultured Purkinje cells. To avoid potential developmental compensations, here we adopted the CRISPR/Cas9-based genome editing approach, rather than using global knock out mice. Those GPR55-KO cells, as noted above in response to the comment #2 of reviewer #1, showed decreased fluorescent labeling of PC axon terminals to fluorescent-variant of AM251 (shown in new Figure 2) and abolishment of AM251-mediated suppression of vesicle exocytosis (Figure 3D and E). These results are explained in the text p5-6, lines 141-159; p6, lines 173-178.

> *(3) Include references supporting AM251 and LPI as GPR55 agonists and specify the E50 concentrations for each agonist. Furthermore, provide details about the GPR55 antagonist CID16600046.*

As suggested, we have added references regarding GPR55 agonists, AM251 and LPI. In the text, the following information was added: AM251, originally characterized as an inverse agonist for CB1, has also been reported to act as a GPR55 agonist (Ryberg et al., 2007; Henstridge et al., 2009) (p5, lines 115-116). LPI is an established endogenous GPR55 agonist (Oka et al., 2007; Henstridge et al., 2009) (p5, lines 127-129). The reported $EC_{50}$ values are ~ 30 nM for LPI (Oka et al., 2007, HEK cell assay) and 39 nM for AM251 (Ryberg et al., 2007, HEK cell assay) (p4, lines 94-95; p5, lines 127-129). Regarding the GPR55 antagonist CID16020046, detailed information ($IC_{50}$ = 0.21 μM for GPR55 without significant effect on CB1 receptor) was added in the text with an appropriate citation (Kargl et al., 2013) (p5, lines 123-127). These points have also been added to the Methods section (p17, lines 587-589).

> *(4) Regarding the onset delay (Figure 4C; page 8, lines 3-4), consider the following: "AM251 induced a modest yet significant synaptic delay, estimated by the time to the onset of release" (or something similar).*

We thank the reviewer for suggesting helpful explanation. Accordingly, we have changed the sentence to explain the delayed onset (p9, lines 264-265).

> *These three points should be properly acknowledged in the Discussion:*
>
> *(1) Are action potentials (APs)/depolarizations and ionomycin applications comparable? Ionomycin mediates a large calcium rise significantly slower than the calcium rise mediated by fast depolarization. Such presynaptic calcium dynamics could account, in part, for the different results.*

The qualitative difference of $Ca^{2+}$ increase between APs/depolarization-mediated ones and ionomycin-mediated one is an important point. Thank you for pointing out this issue. In the revised manuscript, we have added an explanation about the possible difference arising from the distinct dynamics of $Ca^{2+}$ increases caused by direct depolarization of axon terminals or by ionomycin (p14, lines 452-453).

> *(2) Previous studies on hippocampal CA3-CA1 pyramidal cell synapses indicate that GPR55 activation enhances glutamate release through presynaptic calcium modulation while diminishing inhibitory postsynaptic strength by reducing GABAA receptors (Sylantyev et al., PNAS 2013; Rosenberg et al., Neuron 2023). In contrast, Inoshita and Kawaguchi discovered that GPR35 suppresses PC-DCN inhibitory transmission by decreasing GABA release without affecting inhibitory postsynaptic strength. Some potential explanation for this discrepancy is warranted.*

We appreciate the reviewer for pointing out this important issue, and feel sorry for not providing an appropriate discussion about the possible interpretation in the previous manuscript. In the revised manuscript, we have added explanations for this discrepancy. First, PC terminals show only limited influence by elevated cytoplasmic $Ca^{2+}$ through ER store on GABA release (Gomez et al., 2020) probably due to abundant calbindin. Second, our present data clearly show the GPR55 signals at PC terminals (although indirect, see Figure 2), while hippocampal inhibitory neuronal boutons somehow showed lower GPR55 levels compared with excitatory neuronal boutons (Rosenberg et al., Neuron, 2023). Third, the subtypes and/or anchoring mechanism for postsynaptic $GABA_A$ receptors might be different between two distinct postsynaptic neurons in the hippocampus and the cerebellum. These factors are now clearly discussed in the text (p12, lines 380-396).

> *(3) Earlier work has suggested that CB1 receptor activation can alter the release machinery. Therefore, the observation that GPR55 activation induces changes in the RRP is not entirely surprising.*

As pointed out, previous studies showed that CB1R influences the synaptic release machinery, rather than $Ca^{2+}$ influx (Ramirez-Franco et al., 2014). In that context, as the reviewer says, the GPR55-mediated RRP change can be regarded as a similar synaptic modulation mechanism as the CB1-mediated one. However, considering the different downstream signaling pathways, $G_{12/13}$- or $G_q$-mediated one and $G_{i/o}$-mediated one, our findings would provide an important scope about the regulation mechanisms of release machinery, which should be further analyzed in the future study. Now we have added these points in discussion (p13-14, lines 435-439).

> *(4) Add a section about the limitations of this study (see Weaknesses above).*

As suggested, we have added a section about the limitations of this study at present, which we could not address in the revision and should be addressed in the future (p15, lines 488-508). Particularly, the actual endogenous agonist to activate GPR55, and the physiological situation in which the agonist is produced, much more direct evidence for GPR55 presence at PC

boutons, and the downstream mechanisms of GPR55-mediated suppression of GABA release are now clearly notified in that section.

> *(5) Double-check grammar and typos ("anandamid").*

We are really sorry for the poor writings in the previous manuscript. Now, we have carefully checked the text.

https://doi.org/10.7554/eLife.105268.2.sa0